iScience

CellPress
OPEN ACCESS

Article

LGP2 is essential for zebrafish survival through dual regulation of IFN antiviral response

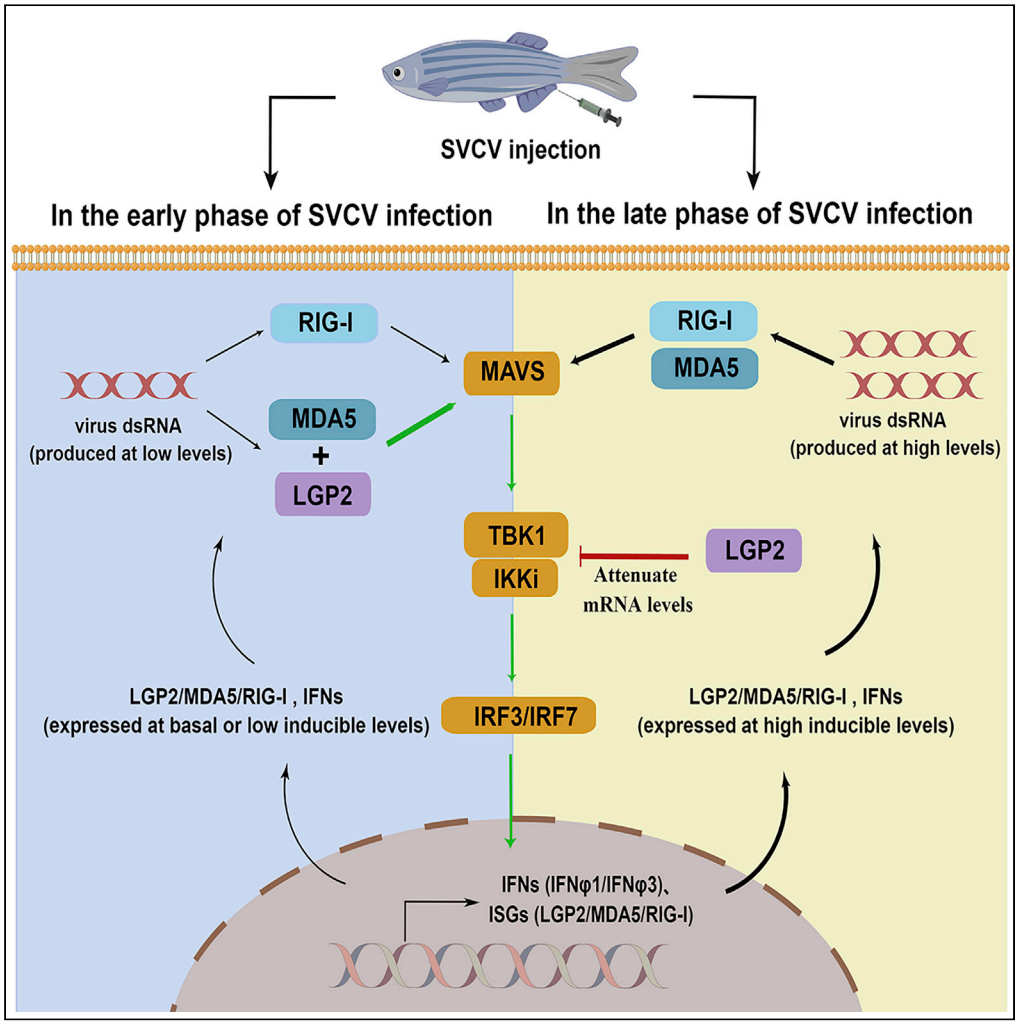

Xiu-Ying Gong, Qi-Min Zhang, Xiang Zhao, ..., Cheng Dan, Jian-Fang Gui, Yi-Bing Zhang

ybzhang@ihb.ac.cn

Highlights

Zebrafish LGP2 is crucial for host survival through initiating IFN response

Zebrafish LGP2 exerts dual regulation of IFN response during SVCV infection

The function switch of zebrafish LGP2 is related to cellular IFN production

Gong et al., iScience 25, 104821
August 19, 2022
https://doi.org/10.1016/j.isci.2022.104821

iScience

CellPress
OPEN ACCESS

Article

LGP2 is essential for zebrafish survival through dual regulation of IFN antiviral response

Xiu-Ying Gong,[1,2] Qi-Min Zhang,[1,2,4] Xiang Zhao,[1,2] Yi-Lin Li,[1,2] Zi-Ling Qu,[1,2] Zhi Li,[1] Cheng Dan,[1,2] Jian-Fang Gui,[1,2,3] and Yi-Bing Zhang[1,2,3,5,*]

SUMMARY

In mammals, LGP2 is the enigmatic RLR family member, being initially believed as an inhibitor of RLR-triggered IFN response but subsequently as an activator of MDA5 signaling and an inhibitor of RIG-I signaling. The contradiction happens to fish LGP2. Here, we generate a *lgp2* loss-of-function (*lgp2*$^{lof/lof}$) zebrafish mutant, which is highly susceptible to SVCV infection, displaying an initially decreased activation of IFN response and a following increased one. Mechanistically, zebrafish LGP2 functions as the essential activator of IFN response dependent on MDA5 at the early stage of viral infection but as a negative regulator by impairing mRNA levels of *tbk1* and *ikki* at the late stage of viral infection. The function switch of LGP2 is related to cellular IFN production during viral infection. Our data demonstrate that zebrafish LGP2 is a key homeostatic regulator of IFN response and thus essential for zebrafish survival against SVCV infection.

INTRODUCTION

In mammals, innate immunity to virus infection includes the production of type I interferons (IFNs) that provide the first line of antiviral defense for host survival. IFNs restrict viral replication and dissemination through upregulation of hundreds of IFN-stimulated genes (ISGs), as evidenced by the fact that some ISGs encode antiviral effectors directly, facilitating viral infection clearance (Rehwinkel and Gack, 2020). Although essential for controlling virus replication, cellular IFN production is precisely regulated, as less production cannot clear virus infection thoroughly, and instead, overproduction results in host autoimmune diseases and chronic inflammatory responses. Accordingly, some other ISGs play positive or negative roles in fine-tuning IFN signaling cascades (Rehwinkel and Gack, 2020).

IFN response is often initiated through sensing virally derived nucleic acids in the cytosol of infected cells by retinoic acid-inducible gene-I (RIG-I)-like receptors (RLRs), including RIG-I, MDA5 (melanoma differentiation-associated gene 5), and LGP2 (laboratory of genetics and physiology 2, also known as DHX58) (Rehwinkel and Gack, 2020). RIG-I and MDA5 share similar domain organizations, consisting of two N-terminal caspase activation and recruitment domains (CARDs), a central DExD/H-box RNA helicase domain and a C-terminal regulatory domain (CTD). Sensing viral RNA substrates by CTD and helicase domain of RIG-I and MDA5 facilitates structural rearrangements, thus releasing N-terminal CARDs from an autoinhibitory state, which enables oligomerization and activation of MAVS (mitochondrial antiviral signaling protein), an adaptor possessing N-terminal CARDs (Duic et al., 2020; Rehwinkel and Gack, 2020). MAVS recruits protein kinases TBK1 (TANK-binding kinase 1) and IKKε (inhibitor of nuclear factor kappa B kinase subunit epsilon, or IKKi) to phosphorylate and activate IFN regulatory factors 3/7 (IRF3/7), driving the expression of IFN and subsequent ISGs for host antiviral state (Rehwinkel and Gack, 2020).

Similar to RIG-I and MDA5, LGP2 has strong binding affinities to viral dsRNA, although the precise features of RNA are less well defined (Rehwinkel and Gack, 2020). Unlike RIG-I and MDA5, LGP2 lacks the N-terminal CARDs that are required for signaling transmission to MAVS. As a typical ISG, LGP2 is initially believed as a feedback inhibitor of IFN response (Yoneyama et al., 2005). *In vitro* studies showed that LGP2 downregulates RIG-I signaling, likely through prevention of MAVS from association with RIG-I (Esser-Nobis et al., 2020; Saito et al., 2007) or with IKKi (Komuro and Horvath, 2006), sequestration of viral dsRNA away from RIG-I (Rothenfusser et al., 2005), and inhibition of RIG-I ubiquitination by targeting TRIM25 (Quicke et al., 2019). On the other hand, a series of studies indicated that LGP2 coordinates MDA5 but impairs RIG-I to augment IFN response while a common signaling cascade is shared by MDA5 and RIG-I

[1]State Key Laboratory of Freshwater Ecology and Biotechnology, Institute of Hydrobiology, Chinese Academy of Sciences, Wuhan 430072, China

[2]University of Chinese Academy of Sciences, Beijing 10049, China

[3]The Innovation Academy of Seed Design, Chinese Academy of Sciences, Wuhan 430072, China

[4]Present address: College of Life Science and Technology, National Engineering Research Center for Nanomedicine, Huazhong University of Science and Technology

[5]Lead contact

*Correspondence: ybzhang@ihb.ac.cn

https://doi.org/10.1016/j.isci.2022.104821

(Bruns et al., 2013, 2014; Childs et al., 2013; Duic et al., 2020; Pippig et al., 2009; Sanchez David et al., 2019), RNA binding is required for LGP2 to be a positive regulator but not for its negative role (Bamming and Horvath, 2009; Bruns et al., 2013, 2014; Childs et al., 2013; Satoh et al., 2010; Uchikawa et al., 2016), and RIPLET rather than TRIM25 is essential for RIG-I signaling (Cadena et al., 2019). The controversial data cannot perfectly interpret LGP2's roles in RLR-mediated signaling (Bruns and Horvath, 2015; Rehwinkel and Gack, 2020).

In vivo studies exacerbate the aforementioned contradiction. Three separate strains of *lgp2*$^{-/-}$ mice have different phenotypes (Satoh et al., 2010; Suthar et al., 2012; Venkataraman et al., 2007). The first knockout mice exhibit resistance to VSV infection (recognized by RIG-I) and sensitivity to EMCV infection (recognized by MDA5) (Venkataraman et al., 2007), but the second deficient mice are highly vulnerable to RNA viruses recognized by both RIG-I and MDA5 (Satoh et al., 2010). Delineation of the third strain illustrates that LGP2 is not essential for IFN response but rather regulates T cell function during viral infection (Suthar et al., 2012). Despite these differences, the former two *lgp2*$^{-/-}$ mice are susceptible to EMCV infection, indicating that LGP2 is a positive regulator of MDA5 signaling, as suggested by *in vitro* experiments (Childs et al., 2013; Pippig et al., 2009). In addition, two transgenic mouse modes that overexpress human LGP2 exhibits a diminished IFN response and a reduced viral load (Chopy et al.; Si-Tahar et al., 2014), still showing ambivalent roles of LGP2 during innate immune response to virus infection.

Teleost fish have orthologs of three RLR receptors and downstream molecules (MAVS, MITA, TBK1, IRF3, and IRF7), all of which exert similar functions in mammals (Bergan et al., 2010; Biacchesi et al., 2012; Chang et al., 2011; Iliev et al., 2011; Sun et al., 2010, 2011; Zhang et al., 2014; Zhang and Gui, 2012). Surprisingly, *in vitro* assays have shown contradictory roles of fish LGP2 in IFN response (Chang et al., 2011; Liu et al., 2017a; Ohtani et al., 2010; Rao et al., 2017; Sun et al., 2011; Yu et al., 2016). Our *in vitro* data suggested that zebrafish LGP2 exerts dual function in response to viral infection (Zhang et al., 2018). To better understand the exact role of zebrafish LGP2 in fish IFN response, we generated a zebrafish mutant where *lgp2* is loss of function (LoF) and found that the zebrafish mutant (*lgp2*$^{lof/lof}$) is hypersensitive to SVCV infection. *Lgp2*$^{lof/lof}$ zebrafish exhibits a reduced induction of IFN response at the early phase of SVCV infection but an enhanced one at the late phase; the function switch of zebrafish LGP2 occurs when the cellular IFNs are produced to a threshold level. Finally, zebrafish LGP2 functions as a positive regulator dependent on MDA5 and a negative one by impairing *tbk1* and *ikki* mRNA levels. Our results indicate that zebrafish LGP2 is a key homeostatic regulator of IFN response during virus infection.

RESULTS

LGP2 deficiency impairs zebrafish survival against SVCV infection

TALEN technique was used to target a 15-bp spacer DNA within the exon 10 of zebrafish *lgp2* gene (Figure S1A). Sequencing confirmed a mutant line with seven base mutations and a single base deletion at the TALEN site, thus generating a truncated protein, LGP2-talen (Figure S1B). LGP2-talen is 530aa in length due to lack of the C-terminal RD domain of wild-type (WT) LGP2 (Figure S1C). RT-PCR showed that compared with WT zebrafish, the zebrafish mutant exhibited attenuated constitutive expression of *lgp2* in head kidney, liver, spleen and gill (Figure 1A), and SVCV infection induced a significantly induction of *lgp2-wt* in WT zebrafish but a marginal one of *lgp2-talen* in the zebrafish mutant (Figure 1B). Using a LGP2-specific Ab that was made by a fragment (192–417aa) of zebrafish LGP2 protein (Figures S1D–S1F), western blots revealed a detectable level of LGP2 protein in gill of *lgp2*$^{+/+}$ zebrafish, a marginal one in heterozygous mutant (*lgp2*$^{lof/+}$), and no detection in homozygous mutant (*lgp2*$^{lof/lof}$) (Figure 1C). These results indicated that we have successfully obtained a zebrafish mutant line in which LGP2 might be loss of function (LoF).

Zebrafish larvae (6 dpf) were immersed with SVCV (2×10^6 $TCID_{50}$/mL), and 2 days later, there were 40 survivals out of 50 WT larvae, compared with only 14 survivals for knockout larvae (Figure 1D). Zebrafish larvae started to die at 1 day postinfection (5×10^5 $TCID_{50}$/mL), and no *lgp2*$^{lof/lof}$ larvae was alive at 5 days postinfection, in contrast to nearly 50% WT survivals (Figure 1E). Similarly, wild-type zebrafish adults (60 dpf) showed a higher survival rate than *lgp2*$^{lof/lof}$ adults at 6 days after i.p. injection with SVCV (1×10^8 $TCID_{50}$/mL) (86% versus 0%) (Figure 1F). Along with infection time, *lgp2*$^{lof/lof}$ larvae exhibited a high mRNA expression of SVCV genes over WT larvae (Figure 1G), which was observed in gill, spleen, head kidney, trunk kidney, and liver of *lgp2*$^{lof/lof}$ zebrafish adults (Figure 1H). These results indicated that LGP2 is essential for zebrafish survival against SVCV infection.

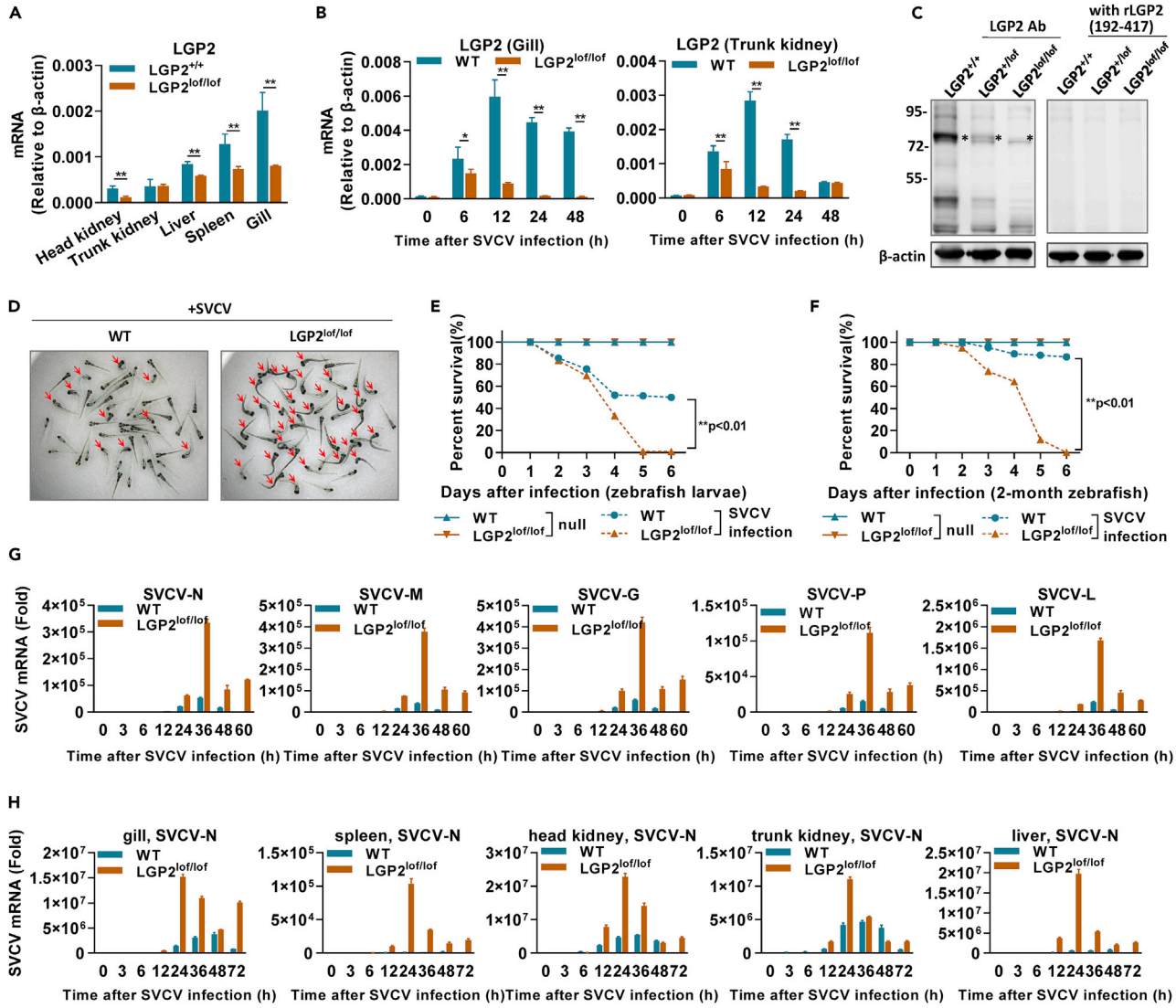

Figure 1. LGP2 deficiency impairs zebrafish survival against SVCV infection

(A and B) RT-PCR detection of *lgp2* (or *lgp2*-talen) mRNA in the indicated tissues from *lgp2*$^{+/+}$ and *lgp2*$^{lof/lof}$ zebrafish adults (60 dpf) in healthy state (A) or following i.p. injection with SVCV (10^8 $TCID_{50}$/mL) (B).

(C) Western blot analysis of LGP2 protein in the gill from *lgp2*$^{+/+}$ and *lgp2*$^{lof/lof}$ zebrafish (120 dpf) by with LGP2 antibody. * indicated the LGP2 protein band. The bands below * were nonspecific proteins.

(D) Representative imaging of *lgp2*$^{+/+}$ and *lgp2*$^{lof/lof}$ zebrafish larvae (6 dpf, n = 50) immersed with SVCV (2×10^6 $TCID_{50}$/mL) for 2 d. Red arrows indicated the dead larvae. (E and F) Mortality analysis of *lgp2*$^{lof/lof}$ larvae (E) and adults (F) together with WT zebrafish following SVCV infection.

(E) *lgp2*$^{+/+}$ and *lgp2*$^{lof/lof}$ zebrafish larvae (6 dpf, n = 100) were immersed with SVCV (5×10^5 $TCID_{50}$/mL).

(F) *lgp2*$^{+/+}$ and *lgp2*$^{lof/lof}$ zebrafish adults (60 dpf, n = 50) were injected i.p. with SVCV (10^8 $TCID_{50}$/mL), at 20 μL per fish.

(G and H) LGP2 deficiency exacerbated SVCV replication in zebrafish larvae (G) and adults (H). *lgp2*$^{lof/lof}$ larvae (6 dpf) and adults (60 dpf) together with WT zebrafish were infected with SVCV as in (E) and (F), respectively. The expression of five SVCV genes, including nucleoprotein (N), phosphoprotein (P), matrix protein (M), glycoprotein (G), and RNA polymerase (L) was detected by RT-PCR. Data were shown as mean ± SD (N = 3). P values were calculated using Student's t test. *p < 0.05, **p < 0.01. See also Figure S1, and Table S1.

lgp2$^{lof/lof}$ zebrafish exhibits a reduced induction of IFN response at the early phase of SVCV infection but an increased one at the late phase

To evaluate the change of IFN response by LGP2 deficiency, we compared mRNA expression of two *ifn* genes (*ifnφ1* and *ifnφ3*) and three ISGs (*mxb*, *irf3*, and *irf7*) between *lgp2*$^{lof/lof}$ and WT larvae following SVCV infection. All genes had a basal expression and were induced by SVCV infection (Figure 2A, left

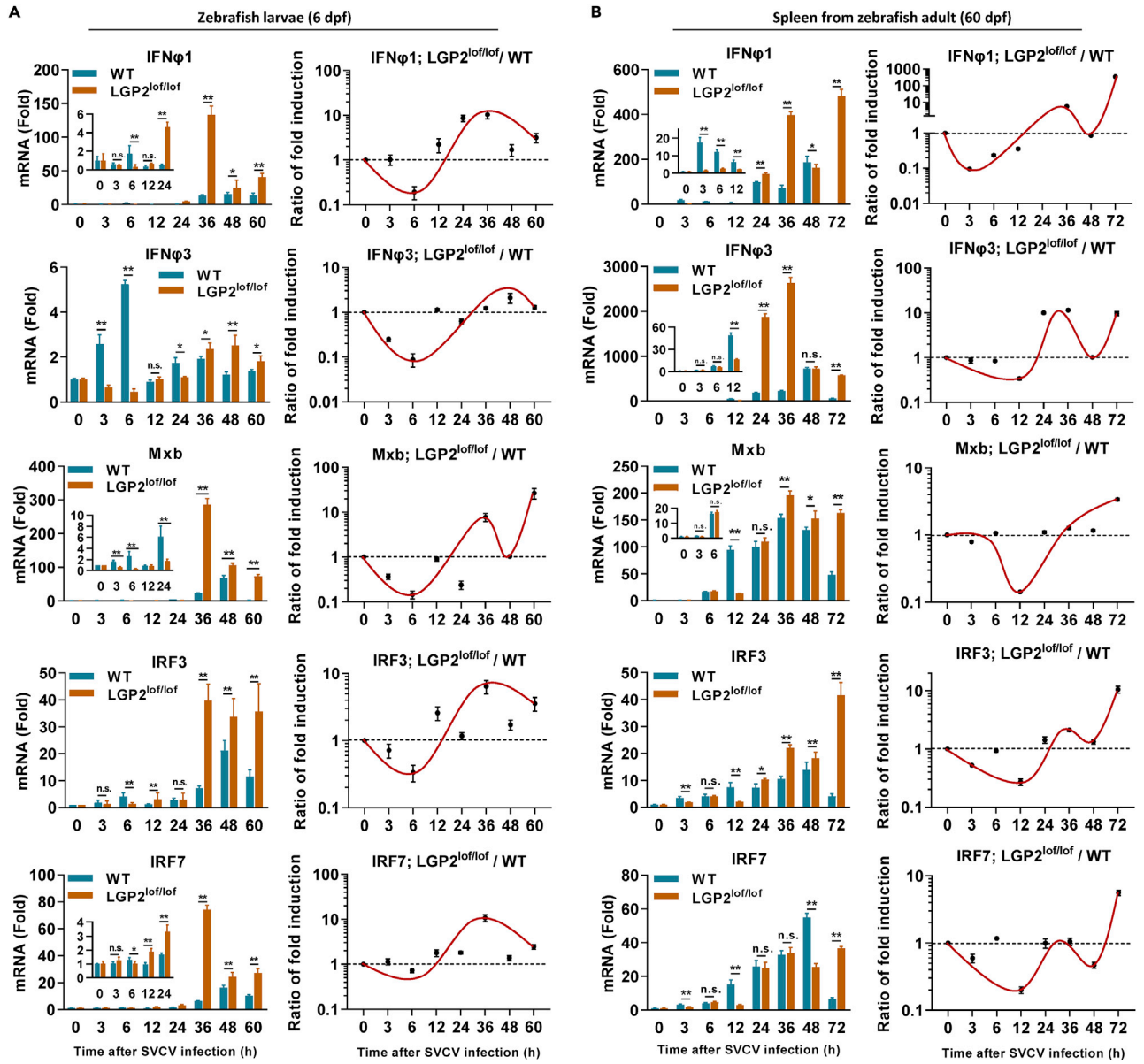

Figure 2. LGP2 promotes IFN response at the early phase of SVCV infection but attenuates at the late phase

(A) mRNA expression comparison of two *ifn* genes and three ISGs between *lgp2*$^{+/+}$ and *lgp2*$^{lof/lof}$ zebrafish larvae following SVCV infection. Left panels: *lgp2*$^{+/+}$ and *lgp2*$^{lof/lof}$ zebrafish larvae (6 dpf) were immersed with SVCV (5×10^5 $TCID_{50}$/mL) for the indicated time points, followed by RT-PCR detection of the mRNA levels of *ifnφ1*, *ifnφ3*, *mxb*, *irf3*, *and irf7*. The expression values were expressed as fold induction relative to that in mock-infected larvae following normalization to *β-actin*. Right panels: the induction ratio of each gene between *lgp2*$^{lof/lof}$ and WT larvae was calculated based on the fold induction at the same time point, followed by normalization to the ratio at 0 h postinfection, which was set to 1, indicating no change.

(B) mRNA expression comparison of two *ifn* genes and four ISGs in spleens between *lgp2*$^{+/+}$ and *lgp2*$^{lof/lof}$ zebrafish adults following SVCV infection. Left panels: *lgp2*$^{+/+}$ and *lgp2*$^{lof/lof}$ zebrafish adults (60 dpf) were injected i.p. with SVCV (10^8 $TCID_{50}$/mL) for the indicated time points, followed by RT-PCR detection. Right panels: the fold induction ratios of each gene in spleen between *lgp2*$^{+/+}$ and *lgp2*$^{lof/lof}$ zebrafish adults. Data were shown as mean ± SD (N = 3). P values were calculated using Student's t test. *p < 0.05, **p < 0.01; n.s., not significant. See also Figure S2, and Table S1.

panels). Generally, <5-fold induction was detectable until 24 h postinfection (the early phase of SVCV infection), in contrast to >40-fold from 24 to 60 h postinfection (the late phase of SVCV infection), with an exception of *ifnφ3* gene that showed <6-fold induction throughout the infection. Further comparison revealed an attenuated induction in *lgp2*$^{lof/lof}$ larvae compared with WT larvae until 24 h postinfection and an enhanced induction from 24 to 60 h postinfection (Figure 2A, left panels).

The expression alteration of five genes in response to SVCV infection was quantified as the ratio of fold induction at the same time points between *lgp2*$^{lof/lof}$ and WT larvae, followed by normalization to the ratio at 0 h postinfection, which was set to 1, indicating no change (Figure 2A, right panels). It clearly showed that, compared with WT larvae, *ifnφ1* expression was significantly attenuated in *lgp2*$^{lof/lof}$ larvae during the early phase of viral infection, particularly at 6 h postinfection (5-fold lower than WT), then started to increase from 12 h postinfection, and peaked at 36 h postinfection (10-fold higher than WT), indicating that *lgp2* deficiency resulted in a first impaired and a subsequent promoted expression induction of *ifnφ1*. Similar results were seen in *ifnφ3*, *mxb*, *irf3*, and *irf7* (Figure 2A, right panels).

Similar comparison was next performed between *lgp2*$^{lof/lof}$ and WT adults following SVCV infection. All five gene expressions were significantly induced in spleen of *lgp2*$^{lof/lof}$ and WT adults (Figure 2B, left panels); however, *lgp2* deficiency caused an obviously weakened induction during the early phase of infection, particularly at 12 h postinfection, but from 24 to 72 h postinfection, an enhanced induction was generally detected compared with WT adults (Figure 2B, right panels). Most of these genes, particularly *ifnφ1*, displayed a similar expression pattern in gill and head kidney (Figures S2A and S2B). These data together indicated that LGP2 promotes IFN antiviral response during the early phase of viral infection but attenuates IFN response during the late phase of viral infection.

LGP2-talen is not functional in fish IFN response

To exclude a possible role of LGP2-talen in *lgp2*$^{lof/lof}$ zebrafish, we first compared the stimulatory ability of LGP2-wt, LGP2-talen, and LGP2-DH that is devoid of RD and is similar to LGP2-talen in size (Figure 3A). Neither LGP2-talen nor LGP2-DH showed any stimulatory effects, but overexpression of LGP2-wt stimulated a robust luciferase activity of crucian carp IFN promoter-driven luciferase construct (CaIFNpro-luc) (Figure 3B). Notably, LGP2-wt exhibited a strongest potential at a relatively low dose (10 ng in 24-well plates) but a dose-dependent weakened induction at relatively high doses (50 and 200 ng in 24-well plates) (Figure 3B). RT-PCR showed that LGP2-wt, but not LGP2-talen nor LGP2-DH, significantly upregulated the mRNA expression of cellular *ifn* gene (Figure 3C) and four ISGs (*mx*, *viperin*, *irf3*, and *irf7*) (Figure S3), also with a strongest induction at a relatively low dose (40 ng in 6-well plates, corresponding to 10 ng in 24-well plates) and a dose-dependent weakened one at relatively high doses (200 and 800 ng). In addition, overexpression of LGP2-talen and LGP2-DH lost the ability to inhibit poly(I:C)-induced activation of CaIFNpro-luc, which was significantly inhibited by LGP2-wt in a dose-dependent manner (Figure 3D). These results indicated that LGP2-talen is not functional in fish IFN response despite a marginal expression in *lgp2*$^{lof/lof}$ zebrafish.

LGP2 functions as a dual regulator in itself- and virus-induced IFN response

The finding that zebrafish LGP2 provokes a strong IFN response at low doses but a weak one at high doses indicated that an inhibition should happen to LGP2 itself. To this end, titration assays showed that low doses of LGP2 ($\leq$10 ng in 24-well plates) stimulated fish IFN promoters obviously in a dose-dependent manner, up to a peak when 10 ng of LGP2 was transfected; thereafter, the promoter activation was gradually reduced along with LGP2 doses increasing (>10 ng), indicating that the highest promoter activation at 10 ng of LGP2 was indeed inhibited by the extra amount of LGP2, also in a dose-dependent manner (Figure 4A). Similarly, low dose of LGP2 (40 ng in 6-well plates) upregulated cellular PKR and IRF3 proteins, which were diminished when LGP2 doses were increased to 200 and 800 ng (Figure 4B).

Subsequent assays were performed to determine the antithetic role of LGP2 during SVCV infection. IRF3 dimerization was not easily detectable in CAB cells transfected with LGP2 alone; however, a low titer of SVCV stimulated IRF3 dimerization, which was more effectively enhanced by LGP2 at 40 ng than at 800 ng (Figure 4C). A high titer of SVCV yielded a robust IRF3 dimerization, which was markedly diminished by LGP2 at either 40 ng or 1000 ng (Figure 4D). Time titration showed that IRF3 dimerization was not detectable until 12 h postinfection, which was gradually obvious along with LGP2 doses; from 24 to 36 h postinfection, transfection of LGP2 at 40 ng or 1000 ng resulted in reduced IRF3 dimerization relative to SVCV infection alone (Figure 4E). Compared with the control without LGP2 transfection, SVCV-induced expression of cellular genes (*ifn*, *viperin*, and *irf3*) was enhanced in the presence of LGP2 until 24 h postinfection, being a strong promotion by 40 ng of LGP2 and a weak one by 1000 ng; however, at 36 h postinfection, the promotional effect was undetectable (Figure 4F). These results indicated that LGP2 firstly promoted and subsequently attenuated IFN response during viral infection.

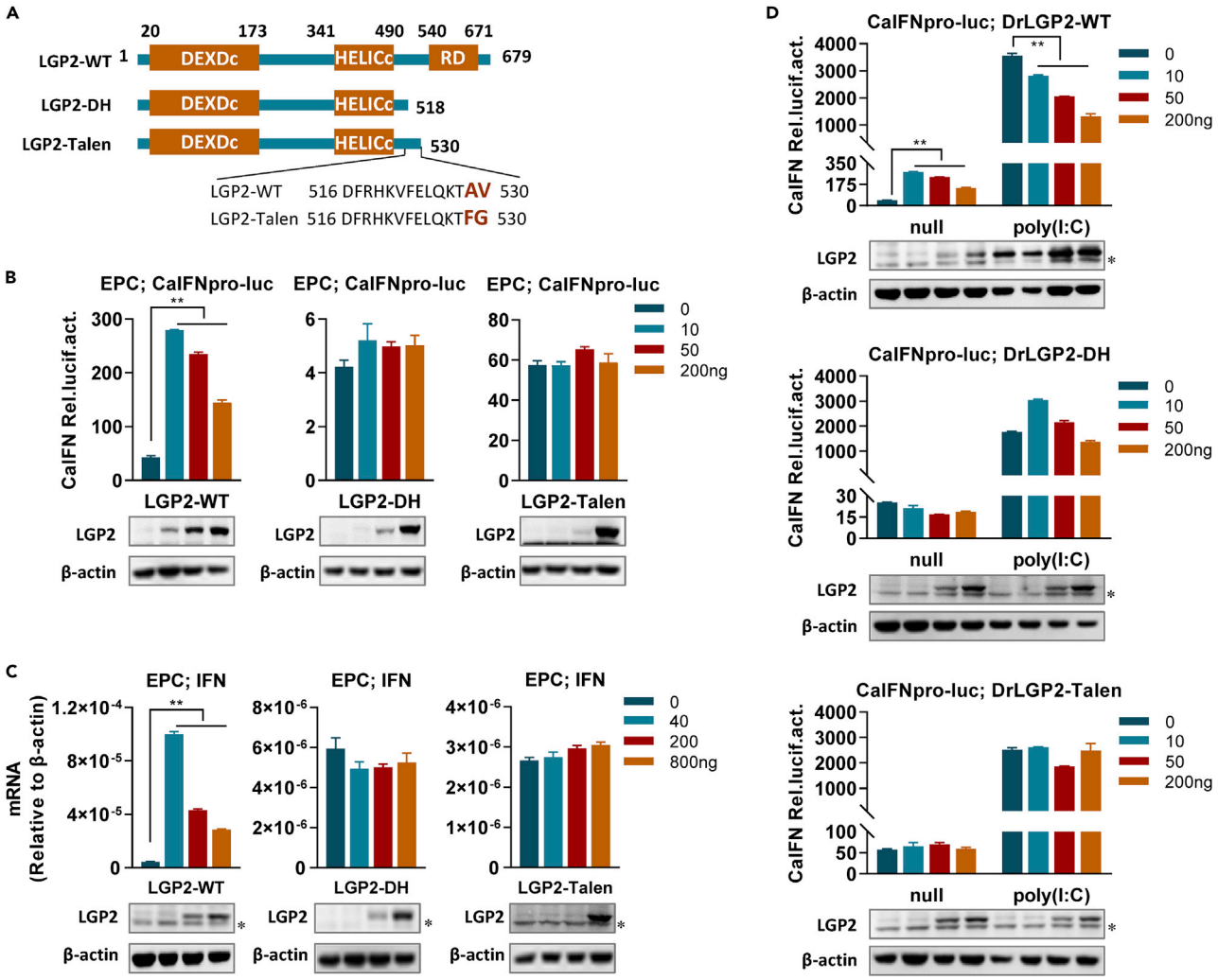

Figure 3. LGP2-talen is not functional in fish IFN response

(A) Schematic of wild-type LGP2 (LGP2-WT), LGP2-talen, and LGP2-DH.

(B) Fish IFN promoter is activated by zebrafish LGP2 but not by LGP2-DH and LGP2-talen. EPC cells seeded in 24-well plates were cotransfected with CalFNpro-luc (200 ng), Renilla vector (pRL-TK, 20 ng), and LGP2-WT/LGP2-DH/LGP2-talen at increasing doses (0, 10, 50, 200 ng) for 48 h, followed by luciferase assays.

(C) Cellular *ifn* gene was not induced by LGP2-talen. EPC cells seeded in 6-well plates were transfected with LGP2-WT, LGP2-DH, or LGP2-talen at increasing amounts (0, 40, 200, 800 ng) for 48 h, followed by RT-PCR.

(D) LGP2-talen failed to inhibit poly(I:C)-triggered IFN response. EPC cells seeded in 24-well plates were transfected for 24 h with 200 ng of CalFNpro-luc and increasing amounts (0, 10, 50, 200 ng) of LGP2-WT or LGP2-talen or LGP2-DH, followed by transfection again with poly(I:C) (1 μg/mL). Another 24 h later, luciferase assays were performed. Western blots in (B), (C), and (D) showed the ectopically expressed LGP2 in a dose-dependent manner by zebrafish LGP2 antibody. *Nonspecific band. Data were shown as mean ± SD (N = 3). P values were calculated using Student's t test. **$p < 0.01$. See also Figure S3 and Table S1.

Function switch of LGP2 is related to IFN production but not to IFN signaling

We hypothesized that zebrafish LGP2 switches its function roles as a result of the cellular IFN expression levels. Transfection of dominant negative mutant plasmids of RLR signaling factors, including RIG-I-DN, MDA5-DN, MAVS-ΔTM, MITA-CT, TBK1-K38M, IRF3-DN, and IRF7-DN, could efficiently block SVCV infection, which triggers IFN response in fish cells (Figure S4A). Next, we compared fish IFN promoter activation by titration of LGP2 from 0 to 200 ng in the absence or presence of these dominant negative mutants (Figure 5A). Similarly, overexpression of LGP2 induced a dose-dependently positive regulation at low doses (≤10 ng) and a dose-dependently negative regulation at high doses (>10 ng). In the presence of MITA-CT, TBK1-K38M, IRF3-DN, or IRF7-DN, the positive regulatory trend triggered by low doses of

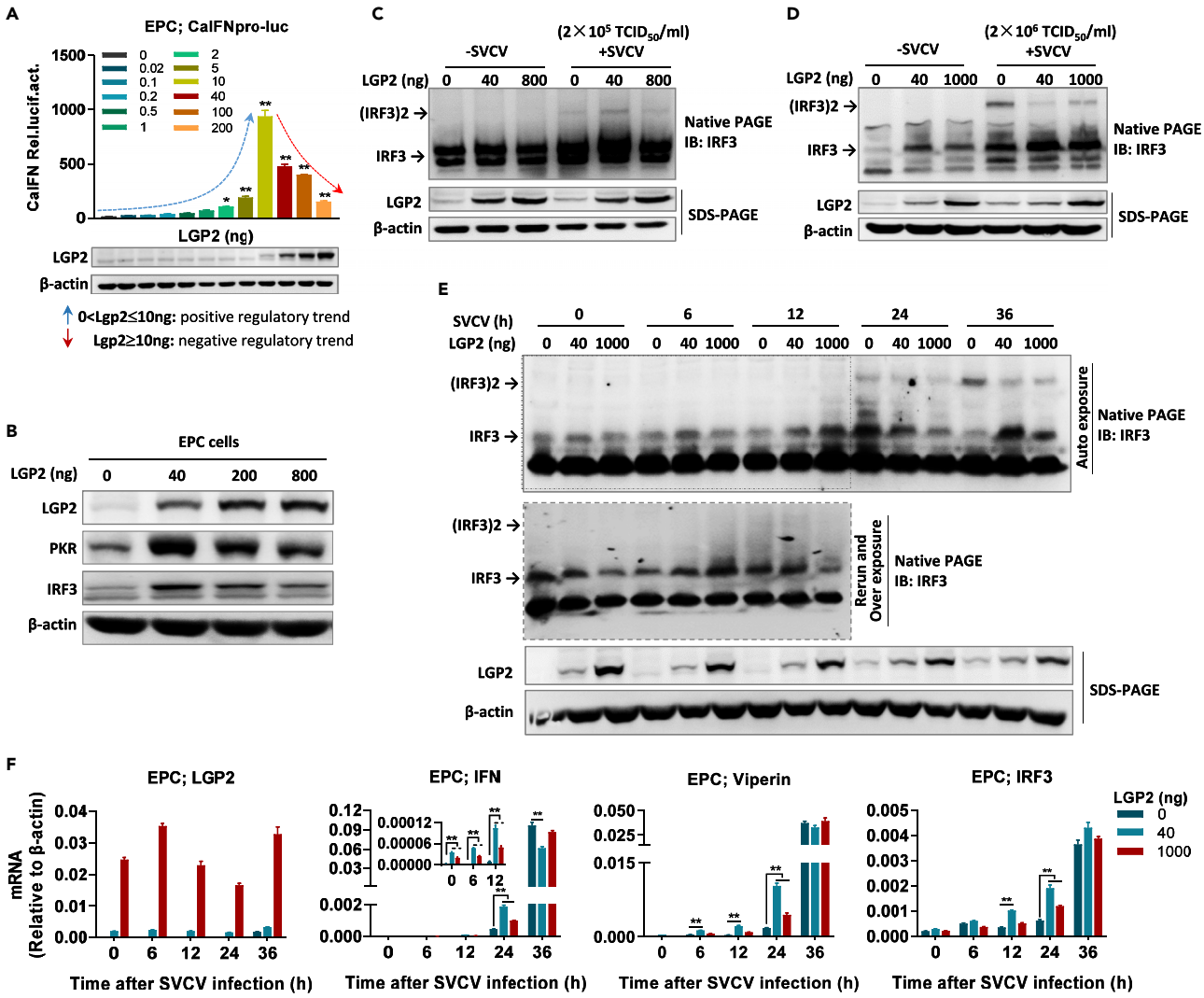

Figure 4. LGP2 functions as a dual regulation of itself- and virus-induced IFN response

(A and B) LGP2 played antithetic role in itself-induced fish IFN promoter activation (A) and upregulation of IFN-inducible proteins (B). EPC cells seeded in 24-well plates (A) or 6-well plates (B) were transfected with LGP2 at the indicated doses for 48 h, followed by luciferase assays (A) or by western blot detection of PKR, IRF3, and LGP2 with corresponding antibodies (B). Western blot in (A) showed the ectopically expressed LGP2 in a dose-dependent manner by zebrafish LGP2 antibody.

(C and D) IRF3 dimerization was analyzed in SVCV-infected CAB cells in the absence or presence of LGP2. CAB cells seeded in 6-well plates overnight were transfected with LGP2 at the indicated doses for 24 h, followed by infection with SVCV at a relatively low titer (2×10^5 $TCID_{50}$/mL) (C) or at a relatively high titer (2×10^6 $TCID_{50}$/mL) (D) for another 24 h. The transfected cells were collected to detect IRF3 dimerization by native PAGE with anti-IRF3 Ab.

(E and F) LGP2 exerted an early synergizing and a late inhibitory regulation on *ifn*, *viperin*, and *irf3* mRNA expression along SVCV infection. EPC cells seeded in 6-well plates overnight were transfected with the indicated doses of LGP2 for 24 h, followed by infection with SVCV (2×10^5 $TCID_{50}$/mL). At the indicated time postinfection, cells were collected to detect IRF3 dimerization by native PAGE with anti-IRF3 Ab and LGP2 expression by SDS-PAGE with anti-LGP2 Ab (E) or to detect the expression of *lgp2*, *ifn*, *viperin*, and *irf3* expression by RT-qPCR (F). Data were shown as mean ± SD (N = 3). P values were calculated using Student's t test. *$p < 0.05$, **$p < 0.01$.

LGP2 (≤10 ng) was still seen, albeit to a low degree of induction values, but the negative regulatory trend by high dose of LGP2 alone (>10ng) was undetectable or delayed and even changed to a positive regulatory trend in the presence of TBK1-K38M, IRF3-DN, or IRF7-DN (Figure 5A). Under the same conditions, LGP2 inhibited itself-triggered expression of cellular genes (*ifn*, *mx*, *viperin*, *irf3*, and *irf7*) in a dose-dependent manner; however, this inhibitory trend was abolished and even changed to a promoting trend when RLR-IFN signaling was functionally blocked by these dominant negative mutants (Figures 5B and S4B). Notably, overexpression of MDA5-DN completely blocked LGP2-triggered fish promoter activation

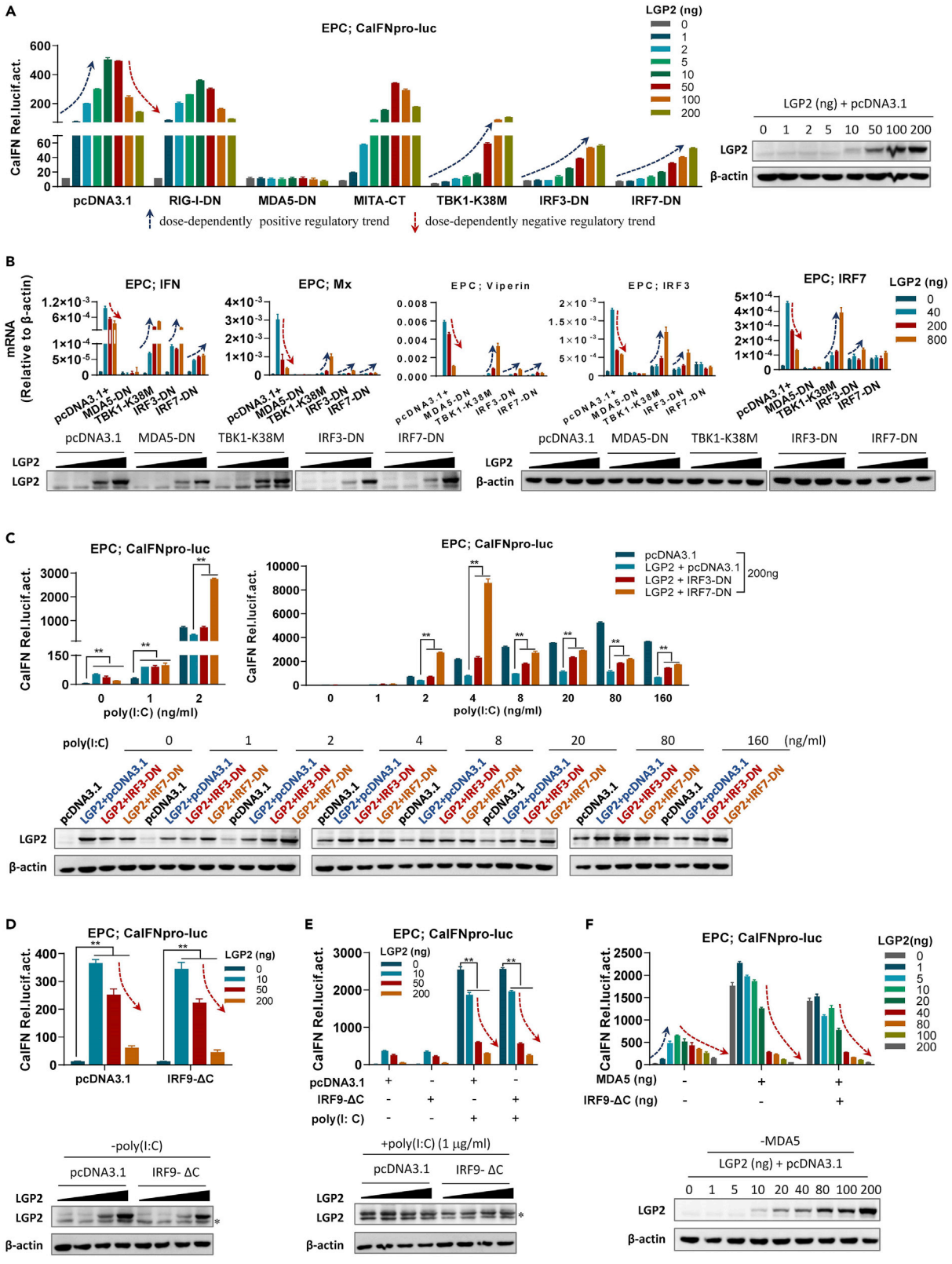
A
EPC; CalFNpro-luc
LGP2 (ng)
0
1
2
5
10
50
100
200
CalFN Rel.lucif.act.
pcDNA3.1
RIG-I-DN
MDA5-DN
MITA-CT
TBK1-K38M
IRF3-DN
IRF7-DN
dose-dependently positive regulatory trend
dose-dependently negative regulatory trend
LGP2 (ng) + pcDNA3.1
LGP2
β-actin
B
EPC; IFN
EPC; Mx
EPC; Viperin
EPC; IRF3
EPC; IRF7
mRNA (Relative to β-actin)
LGP2 (ng)
C
EPC; CalFNpro-luc
poly(I:C) (ng/ml)
pcDNA3.1
LGP2 + pcDNA3.1
LGP2 + IRF3-DN
LGP2 + IRF7-DN
200ng
D
EPC; CalFNpro-luc
IRF9-ΔC
-poly(I:C)
+poly(I:C) (1 μg/ml)
E
EPC; CalFNpro-luc
poly(I: C)
F
EPC; CalFNpro-luc
MDA5 (ng)
IRF9-ΔC (ng)
-MDA5

Figure 5. Function switch of LGP2 is related to IFN production but not to IFN signaling

(A) Luciferase assay analyses of LGP2-triggered fish IFN promoter activation in the absence or presence of the indicated dominant negative mutants of RLR signaling molecules. EPC cells seeded in 24-well plates were cotransfected with CaIFNpro-luc, each of the indicated dominant negative plasmids (200 ng each), together with LGP2 at increasing doses for 48 h.

(B) LGP2-directed mRNA expression of cellular genes was suppressed by functional blockade of RLR signaling. EPC cells seeded overnight in 6-well plates were transfected with each of the indicated dominant negative plasmids (800 ng), together with LGP2 at increasing amounts for 48 h, followed by RT-PCR detection of *ifn*, *mx*, *viperin*, *irf3*, and *irf7* transcripts.

(C) Antithetic effects of LGP2 on poly(I:C)-triggered fish IFN promoter activation in the absence or presence of IRF3-DN or IRF7-DN by luciferase assays. EPC cells seeded in 24-well plates were transfected with CaIFNpro-luc and LGP2, together with IRF3-DN or IRF7-DN (200 ng each) for 24 h, followed by transfection again with poly(I:C) at increasing concentrations (from 0 to 160 ng/mL) for another 24 h.

(D–F) Function blockade of IRF9 did not impair LGP2-triggered negative regulatory trend in the presence of LGP2 self (D), poly(I:C) (E), and MDA5 (F). EPC cells seeded in 24-well plates were transfected as in (A) with the indicated plasmids for 24 h (D and F) followed by luciferase assays or transfected again with poly(I:C) (1 μg/mL) for another 24 h (E) followed by luciferase assays. IRF9-ΔC and MDA5 was transfected at 200 ng. Western blot in (A–F) showed the ectopically expressed LGP2 in a dose-dependent manner by anti-LGP2 Ab, and it is noted that the endogenous LGP2 was also induced by poly(I:C) in (E). *Nonspecific band. Data were shown as mean ± SD (N = 3). P values were calculated using Student's t test. **$p < 0.01$. See also Figure S4 and Table S1.

(Figure 5A) and the mRNA expression of cellular *ifn* and ISGs (Figure 5B), indicating that MDA5 is essential for LGP2 regulation of IFN response.

Subsequently, luciferase assays showed that, compared with the control transfected with pcDNA3.1, low doses of poly(I:C) (<2 ng/mL)-triggered fish promoter activation was significantly promoted by LGP2, which was still observed in the presence of IRF3-DN or IRF7-DN (Figure 5C, left panel). High doses of poly(I:C) (≥2 ng/mL)-triggered promoter activation was markedly inhibited by LGP2; however, this inhibition could be rescued in the presence of IRF3-DN or IRF7-DN, to different extents (Figure 5C, right panel). Moreover, functional blockade of IFN-triggered JAK-STAT signaling by overexpression of IRF9-ΔC, a dominant negative mutant of IRF9 (Yu et al., 2010), could not rescue LGP2-mediated negative regulatory trend, which always occurred in the presence of high doses of LGP2 itself (Figure 5D), poly(I:C) (Figure 5E), and MDA5 (Figure 5F). These results together indicated that cellular IFN expression is a key factor to determine the function switch of zebrafish LGP2 during viral infection.

LGP2 positively regulates fish IFN response dependently of MDA5

To corroborate the finding that MDA5 is essential for LGP2 regulation of IFN response (Figures 5A and 5B), we compared the effects of different dominant negative mutants of RLR molecules on cellular IRF3 and IRF7 expression. Western blots showed that IRF3 and IRF7 proteins were significantly upregulated in fish cells by transfection of LGP2 alone at a low (250 ng) or high dose (5 μg), as compared with the control (lane 6 versus lane 1 in Figure 6A); however, this upregulation was suppressed to different extents by individual cotransfection of RIG-I-DN, MDA5-DN, MAVS-ΔTM, and MITA-CT, with the most severe suppression by MDA5-DN (lane 8 versus lanes 6–7 and 9–10 in Figure 6A), highlighting the relevance of MDA5 to LGP2-directed IFN signaling.

Further fractionation of nucleus and cytoplasm showed that overexpression of LGP2 alone, regardless of the doses transfected, resulted in a robust nuclear accumulation of IRF3 and IRF7, which was always attenuated by simultaneous overexpression of MDA5-DN (Figure 6B). As an IFN-inducible protein, cellular LGP2 expression was also inhibited particularly by overexpression of MDA5 (Figures 6A–6C). Notably, three forms of IRF3 proteins were detected in cytoplasm (Figure 6C), and only the largest one, representing a phosphorylated form of IRF3 (Bergan et al., 2010; Feng et al., 2016; Iliev et al., 2011; Sun et al., 2010), was detected in nucleus (Figure 6B), implying that the phosphorylated IRF3 and IRF7 were transported from cytoplasm into nucleus. These results together indicated that LGP2 triggers fish IFN signaling dependently of MDA5.

LGP2 negatively regulates IFN response by attenuating tbk1 and ikki mRNA levels

Luciferase assays showed that overexpression of LGP2 significantly blocked IFN promoter activation by each of the RLR signaling molecules except for IRF3 and IRF7 (Figure 7A). The same is true for mRNA induction of cellular genes (*ifn*, *mx*, and *viperin*) (Figure 7B). Western blot analysis showed that overexpression of LGP2 resulted in reduced protein levels of TBK1 and IKKi, in a dose-dependent manner (Figure S5A) and also in a time-dependent manner (Figure S5B). However, the protein reduction was abolished by the protein synthesis inhibitor cycloheximide (CHX) (Figure 7C), but not by proteasome inhibitor MG132 or lysosome inhibitors NH_4Cl and chloroquine (Figure 7C), indicating that LGP2 cannot downregulate the expression of TBK1 and IKKi at protein levels.

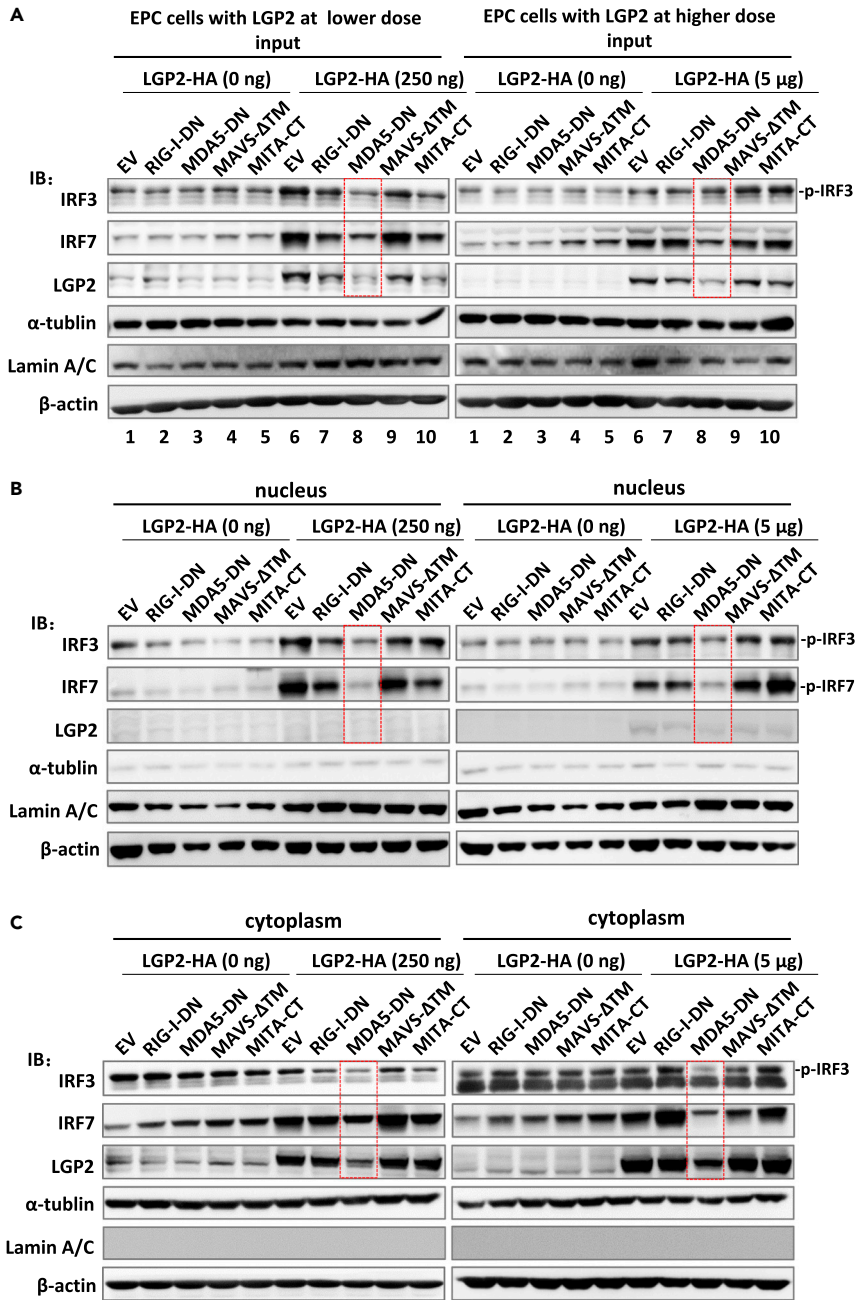

Figure 6. LGP2 positively regulates fish IFN response dependently of MDA5

(A–C) LGP2-directed nuclear accumulation of IRF3 and IRF7 was significantly inhibited by functional blockade of MDA5 signaling. EPC cells seeded in 10-cm dishes were cotransfected with LGP2-HA at a low dose of 250 ng (left panels) or a high dose of 5 μg (right panels), together with the indicated dominant negative mutants (5 μg each). Forty-eight hours later, the transfected cells were harvested for fractionation of the nucleus and cytoplasm. IRF3, IRF7, and LGP2 proteins were detected by western blot analysis of whole-cell lysates as input (A), nuclear extracts (B), and cytoplasmic extracts (C), with antibodies specific to fish IRF3, IRF7, and LGP2, respectively. The red boxes highlighted the essential effects of MDA5-DN on LGP2-triggered signaling.

Further, we evaluated LGP2-mediated expression changes of TBK1 and IKKi at mRNA levels. As shown in Figure 7D, whereas overexpression of LGP2 alone did not nearly change cellular *tbk1* transcript level, overexpression of LGP2 and TBK1 together reduced *tbk1* transcript level, in LGP2's dose-dependent manner, by either vector primers or universal primers, both of which respectively amplified the mRNAs only from the

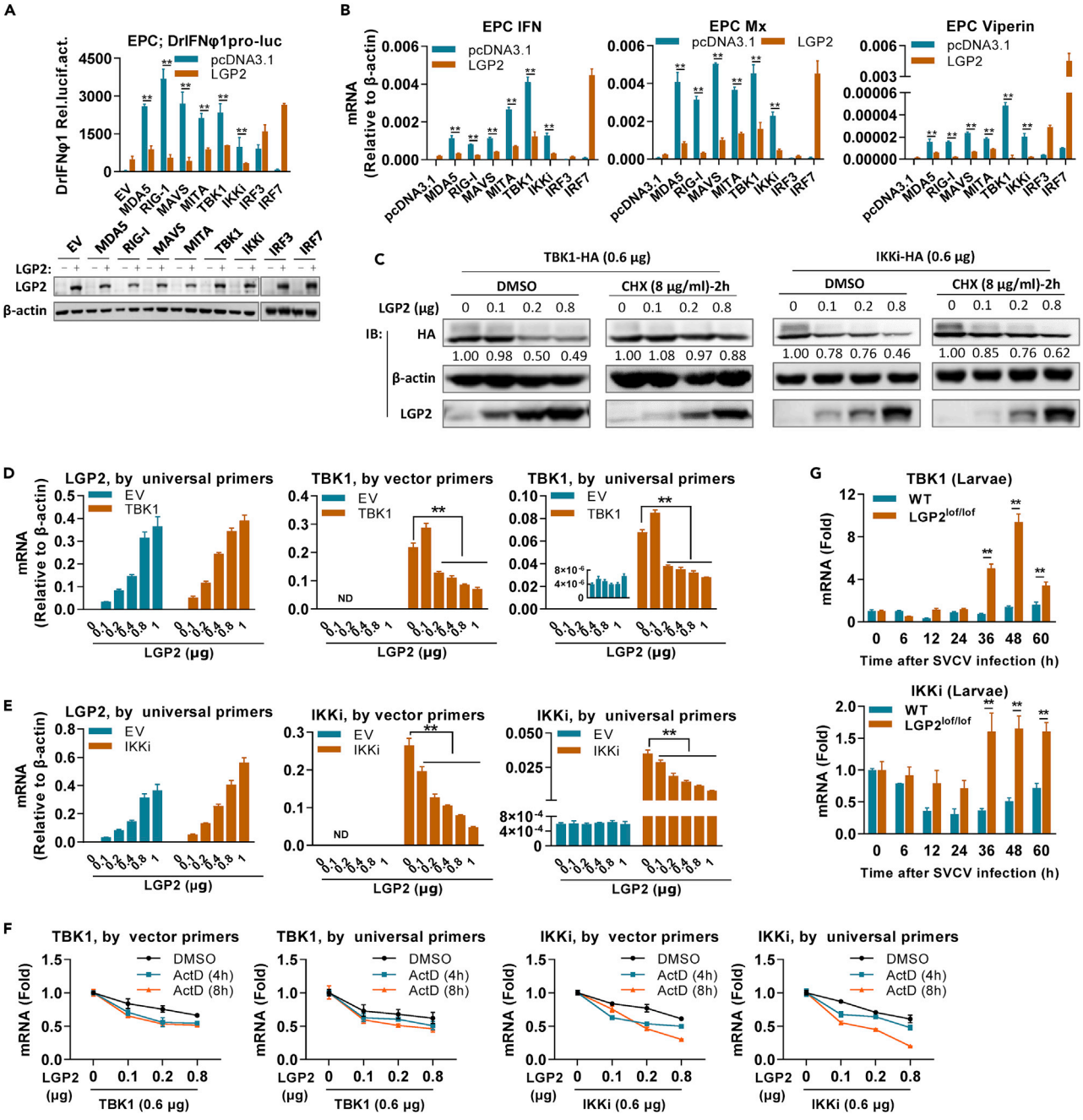

Figure 7. LGP2 negatively regulates IFN response by attenuating tbk1 and ikki mRNA levels

(A and B) LGP2 inhibited fish IFN promoter activation (A) and *ifn* expression (B) induced by RLR signaling molecules upstream of IRF3/7. EPC cells seeded in 24-well plates were transfected with DrIFNφ1pro-luc, LGP2, and each of the indicated RLR signaling molecules (200 ng each) for 48 h, followed by luciferase assays (A) or by RT-PCR detection of cellular *ifn*, *mx*, and *viperin* mRNA (B). Western blots in (A) showed the expression of LGP2 protein in (A and B) by western blots using anti-LGP2 Ab.

(C) LGP2-mediated protein reduction of TBK1 and IKKi was abolished by CHX. EPC cells seeded in 6-well plates overnight were transfected for 24 h with TBK1 or IKKi (0.6 μg each), together with LGP2 at increasing doses, followed by addition of CHX (8 μg/mL) or DMSO as control. Another 2 h later, cells were collected for western blotting analysis of TBK1 and IKKi by anti-HA Ab and LGP2 by anti-LGP2 Ab. The numbers show the densitometric quantification of TBK1 or IKKi protein expression normalized to β-actin.

(D and E) LGP2 attenuated mRNA levels of the transfected TBK1 (D) and IKKi (E). CO cells seeded in 6-well plates were transfected with LGP2 at increasing doses (0, 0.1, 0.2, 0.4, 0.8, 1 μg), together with TBK1 (300 ng, D) or IKKi (300 ng, E) for 48 h, followed by RT-PCR detection of *lgp2*, *tbk1*, and *ikki* mRNA, respectively. Universal primers were designed against the ORF sequences of *tbk1* and *ikki* for detection of mRNA from cellular genes and the transfected

Figure 7. *Continued*

plasmids together, and vector primers only detected mRNA from the transfected plasmids because a forward primer was designed against vector sequences.

(F) LGP2-mediated reduction of *tbk1* and *ikki* mRNA levels was not impaired by ActD. EPC cells seeded in 6-well plates overnight were transfected for 24 h as in (C), followed by addition of ActD (1 μg/mL) or DMSO as control. At 48 h after ActD addition, *tbk1* and *ikki* transcripts were detected by universal primers and vector primers.

(G) The transcript levels of *tbk1* and *ikki* were enhanced in *lgp2*$^{lof/lof}$ zebrafish larvae during the later period of SVCV infection, in contrast to a nearly constant transcript level in WT larvae. The samples were the same as in Figure 2A. Data were shown as mean ± SD (N = 3). P values were calculated using Student's t test. **p < 0.01. See also Figure S5 and Table S1.

transfected constructs expressing *tbk1* or from the cellular *tbk1* and transfected *tbk1* together. The same happened to *ikki* mRNA (Figure 7E). Moreover, the reduction of *tbk1* and *ikki* transcript levels was not impaired by the transcription inhibitor actinomycin D (ActD) (Figure 7F). These results together implied that LGP2 downregulates TBK1 and IKKi expression via attenuating their mRNA levels.

RT-PCR analysis of wild-type zebrafish larvae showed that *tbk1* and *ikki* transcript levels were not nearly changed along with SVCV infection, similar to our previous findings that fish *tbk1* mRNA is not upregulated by IFN and IFN stimuli (Sun et al., 2011); however, *lgp2*$^{lof/lof}$ zebrafish larvae showed a significant upregulation of *tbk1* and *ikki* mRNA levels during the late phase of SVCV infection (Figure 7G). These results indicated that LGP2 is a key homeostatic regulator of *tbk1* and *ikki* expression and that it attenuates *tbk1* and *ikki* mRNA levels to downregulate IFN response during the late stage of viral infection.

LGP2 is essential for IFN response at the early stage of viral infection

To further determine the biological relevance of low doses of LGP2 in fish IFN response, we compared the patterns of IFN induction by LGP2, RIG-I, and MDA5. Unlike zebrafish LGP2, zebrafish RIG-I and MDA5 activated fish IFN promoters exclusively in a dose-dependent manner (Figure 8A). At low doses (5 and 10 ng in 24-well plates), either RIG-I or MDA5 did not show any effects on fish IFN promoter activation; however, LGP2 exhibited dose-dependent stimulatory potential to fish IFN promoters (14- and 60-fold induction over the control) (Figure 8A). At a high dose (200 ng), LGP2 was a poorest stimulator among three RLR members (Figure 8A). Consistently, LGP2 triggered a stronger expression of cellular *ifn* gene than either MDA5 or RIG-I at low doses (20 and 40 ng in 6-well plates) but a weaker one at a high dose (800 ng) (Figure 8B). Combined with the fact that during the early phase of viral infection (<24 h postinfection), RIG-I and MDA5 were expressed at very low levels in zebrafish larvae and tissues (Figure 8C), similar to LGP2 (Figure 1B), these data indicated that zebrafish LGP2 exerts more potential to IFN response than RIG-I or MDA5 at the early stage of viral infection.

DISCUSSION

It is documented that a fully functional adaptive immunity is not well developed in zebrafish until 4 weeks postfertilization (Lam et al., 2004; Traver et al., 2003). This peculiar characteristic makes zebrafish as a useful animal model to study innate antiviral response (Varela et al., 2017), after the first *in vivo* infection mode with SVCV was established (Sanders et al., 2003). LGP2 knockout exacerbates the mortality of zebrafish larvae (6 dpf) following SVCV infection, highlighting that the consequent mortality is ascribed to an impaired zebrafish innate immunity. Similar phenotypes are replicated in zebrafish adults (60 dpf), demonstrating that LGP2 is indispensable for zebrafish resistance to SVCV infection.

Detection of IFN response reveals that zebrafish LGP2 exerts bilateral function during virus infection *in vivo* and *in vitro*. In the early phase of SVCV infection (<24 h postinfection), function loss of LGP2 resulted in a decreased induction of *ifn* and ISGs in zebrafish larvae and adults and instead, an increased one in the late phase of SVCV infection (>24 h postinfection) (Figure 2). Similar results were replicated in cultured fish cells, when infected with SVCV (Figure 4). Obviously, the enhanced IFN response during the late phase of viral infection in *lgp2*$^{lof/lof}$ zebrafish seemed not helpful for viral infection clearance, as zebrafish mutants actually had higher virus loads than WT zebrafish. Therefore, only the IFN-stimulatory potential of zebrafish LGP2 at the early infection is essential for zebrafish survival advantages.

Our data might provide valuable clues to resolve the controversial understanding of LGP2's biological roles in fish and mammals. Supposing the function of LGP2 is largely conserved across vertebrates, it is helpful to understand why LGP2-deficient mice are more susceptible to virus infection than WT mice, because these

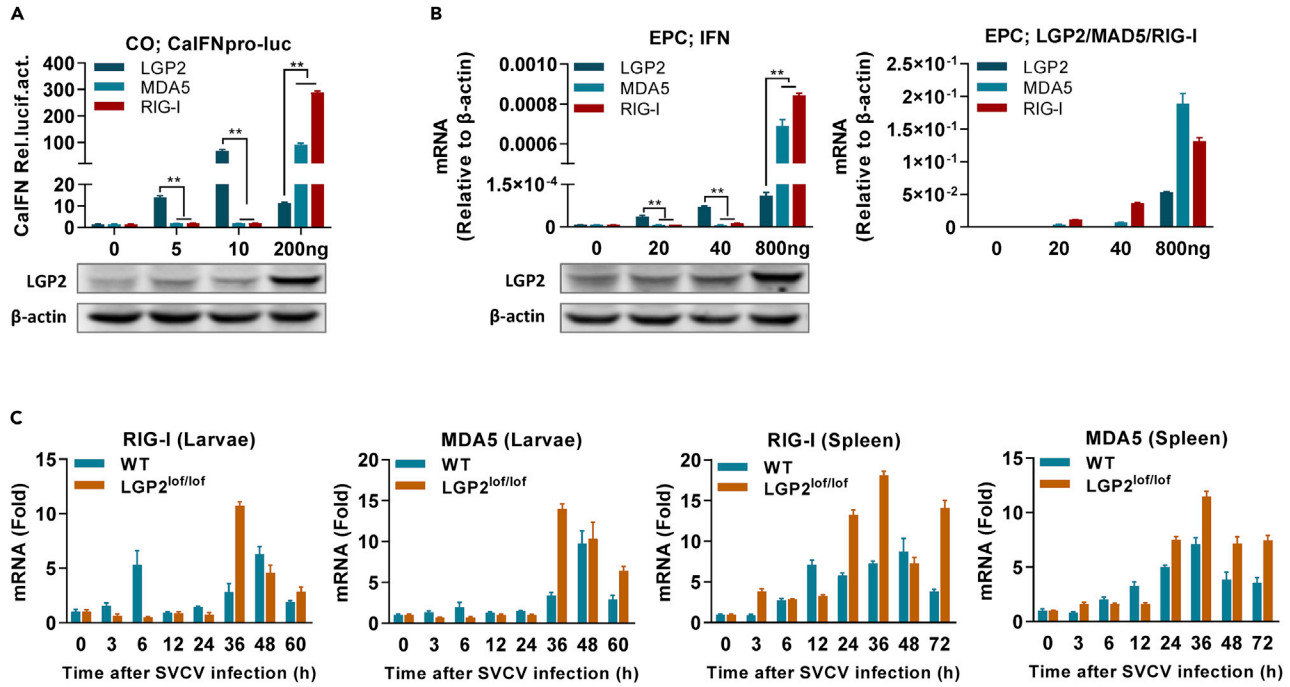

Figure 8. LGP2 is essential for IFN response at the early stage of viral infection

(A) Stimulatory effects of zebrafish LGP2, MDA5, and RIG-I on fish IFN promoter activation by luciferase activity assays. CO cells seeded in 24-well plates were transfected with LGP2, MDA5, and RIG-I at increasing amounts (0, 5, 10, 200 ng) for 48 h. Western blots in (A and B) showed the expression of LGP2 in the transfected cells using anti-LGP2 Ab.

(B) mRNA expression comparison of cellular *ifn* gene by LGP2, MDA5, and RIG-I. EPC cells seeded in 6-well plates were transfected with LGP2, MDA5, and RIG-I at increasing amounts (0, 20, 40, 800 ng) for 48 h, followed by RT-PCR detection of *lgp2* and *ifn* mRNA.

(C) RT-PCR detection of *rig-I* and *mda5* mRNA in $lgp2^{+/+}$ and $lgp2^{lof/lof}$ zebrafish larvae (6 dpf) or in spleen of $lgp2^{+/+}$ and $lgp2^{lof/lof}$ zebrafish adults (60 dpf) following SVCV infection. Data were shown as mean ± SD (N = 3). P values were calculated using Student's t test. **p < 0.01.

mice actually have less IFN production at the early phase of virus infection (within 24 h postinfection) (Satoh et al., 2010); at this time, LGP2 should be expressed at a low level in wild-type mice, thus potentiating IFN antiviral response as the best IFN stimulator of RLRs. It is also easy to understand why two LGP2-transgenic mice have better survival advantages than WT mice, but they display a diminished IFN response and a reduced viral load (Chopy et al., 2011; Si-Tahar et al., 2014). In the latter two studies, endogenous IFN expression was detected during a late phase of virus infection, one from 4 to 8 d postinfection (Si-Tahar et al., 2014) and the other from 8 to 11 d postinfection (Chopy et al.), in which LGP2 functions as a negative regulator of IFN response in mice. Therefore, it is relevant to investigate whether the ectopically expressed LGP2 in the two LGP2-transgenic mice have more IFN production during the early phase of viral infection, a finding as in the current study.

These data reveal that at the beginning of viral infection, it is LGP2 rather than either MDA5 or RIG-I that is responsible for the rapid onset of host IFN response. Fish RIG-I, MDA5, and LGP2 are constitutively expressed at very low levels in tissues of zebrafish at the early phase of SVCV infection. Importantly, LGP2 at low expression levels harbors the best potential to activate IFN antiviral response, and on the contrary, either RIG-I or MDA5 at low expression levels does not nearly exhibit stimulatory effects on fish IFN promoter. It is documented that a rapid initiation of IFN response during the early phase of virus infection is beneficial for host survival (Feng et al., 2021; Gao et al., 2021; Gough et al., 2012). Accordingly, the severe mortality of $lgp2^{lof/lof}$ zebrafish is ascribed to loss of the initial positive regulation of LGP2 during the early phase of infection, and the physiological relevance of LGP2's negative regulation at the late phase of infection might contribute to brake IFN response naturally in wild-type zebrafish, thus ensuring homeostatic regulation of host innate antiviral responses.

Despite no *in vivo* evidence for function switch of LGP2 in mammals, several *in vitro* studies have revealed that lower levels of LGP2 synergize with MDA5 to augment IFN signaling, and higher levels of LGP2 act as

inhibitors of RIG-I and MDA5 signaling (Bruns et al., 2013, 2014; Childs et al., 2013). Correlating with the expression characteristics of LGP2, these data suggested that cellular LGP2 expression level might determine its function switch in RLR signaling (Bruns et al., 2013, 2014; Childs et al., 2013; Pippig et al., 2009). However, we provide solid evidence that zebrafish LGP2, either at lower levels or at higher levels, shows dual effects on the IFN response triggered by SVCV (Figure 4). These results mean that whether zebrafish LGP2 functions as a positive or a negative regulator should be tightly associated with the exact doses or titers of IFN stimuli, rather than the exact expression levels of LGP2 at that time.

Because the exact doses or titers of IFN stimuli, including LGP2 itself at lower levels (<10ng in 24-well plates), are generally proportional to the resultant amounts of IFN products, we hypothesized that a threshold level of cellular IFN production drives the functional switch of zebrafish LGP2 from a positive regulator to a negative one. Evidences come from the LGP2 self-inhibitory model (Figure 5). When RLR signaling was functionally blocked, cellular *ifn* and ISGs expression was inhibited to a low level, and higher doses of LGP2-mediated negative regulation trend was abolished and even changed to a successively positive regulation trend; however, similar phenomenon did not happen when IFN-triggered JAK-STAT signaling was blocked. This means that the function switch of LGP2 is related to IFN production but not to IFN signaling. Therefore, at the early stage of viral infection, SVCV replicates in cells at lower levels, stimulating a lower level of cellular IFN expression; at this time, LGP2, RIG-I, and MDA5 are expressed at lower levels, and LGP2 is most essential for the initiation of IFN response likely dependently of MDA5. At the late stage of infection, SVCV replicates to higher levels, thus inducing cellular IFNs to a threshold level, which switches LGP2 to the negative role.

Although overexpression of LGP2 in human cells cannot activate IFN expression, *in vitro* depletion of PUM1 in HEp-2 cells significantly upregulates the constitutive expression of LGP2, which in turn upregulates the constitutive expression of *ifnb* and some ISGs for host cell survival against virus infection (Liu et al., 2017b), and the constitutively expressed LGP2 might induce IFN response through sensing self RNA and dependently of MDA5 (Stok et al., 2022). These data indicate that human LGP2 at constitutive expression is indeed an essential stimulator of IFN response. Similar to human LGP2, zebrafish LGP2 triggers IFN response with the requirement of MDA5. It is well documented that mammalian LGP2 coordinates fiber formation and subsequent activation of MDA5 (Bruns et al., 2013, 2014; Duic et al., 2020; Esser-Nobis et al., 2020). These results suggest that during the early stage of viral infection, zebrafish LGP2 might facilitate MDA5 activation for the onset of host IFN response.

Limitations of the study

We think that future studies need to further investigate *in vitro* and *in vivo* mechanisms underlying function switch of zebrafish LGP2 using knockout technologies. Recent studies have revealed that human LGP2 enhances apoptosis as an antiviral defense mechanism (Takahashi et al., 2020), and LGP2 downregulates innate immune signaling by inhibiting TRAF ubiquitin ligase (Parisien et al., 2018), blocking the interaction between RIG-I and MAVS (Esser-Nobis et al., 2020), and the K63 conjugating enzyme Ubc13 (Lenoir et al., 2021). However, our results showed that zebrafish LGP2 negatively regulates IFN response likely through attenuating *tbk1* and *ikki* mRNA levels. The transcript levels of *tbk1* and *ikki* are constant in WT zebrafish but significantly upregulated in *lgp2*$^{lof/lof}$ zebrafish, highlighting that zebrafish LGP2 is a key homeostatic regulator to shape IFN signaling toward viral infection. Although the underlying mechanisms of how LGP2 synergizes with MDA5 or impairs mRNA levels of *tbk1* and *ikki* to regulate IFN response are waiting for further clarification using knockout technologies, our results have revealed the *in vivo* bilateral function of zebrafish LGP2 during viral infection, thus providing a clue that similar mechanisms might be involved in mammals.

STAR★METHODS

Detailed methods are provided in the online version of this paper and include the following:

- KEY RESOURCES TABLE
- RESOURCE AVAILABILITY
  - Lead contact
  - Materials availability
  - Data and code availability
- EXPERIMENTAL MODEL AND SUBJECT DETAILS

- Cell lines and cell culture
- Virus strains and experimental models
- METHOD DETAILS
  - Generation of LGP2 mutants by TALEN technique
  - Plasmids
  - Transfection and luciferase activity assays
  - RNA extraction, cDNA synthesis, and quantitative real-time PCR
  - Fractionation of nuclear and cytoplasmic proteins
  - Coimmunoprecipitation and western blotting
- QUANTIFICATION AND STATISTICAL ANALYSIS

SUPPLEMENTAL INFORMATION

Supplemental information can be found online at https://doi.org/10.1016/j.isci.2022.104821.

ACKNOWLEDGMENTS

This work was supported by the grants from the Strategic Priority Research Program of the Chinese Academy of Sciences (XDA24010308), the National Key R&D Program of China (2018YFD0900302), the National Natural Science Foundation of China (31972826, 32102838), and the Application Fundamental Frontier Special Project of Wuhan (2020020601012256). We thank for the instrument help from Wuhan regional center of life science instrument.

AUTHOR CONTRIBUTIONS

Y.B.Z. conceived the project, and Y.B.Z. and X.Y.G. designed the experiments. X.Y.G. performed the majority of the experiments. Q.M.Z. and Z.L. performed *lgp2* knockout zebrafish. Y.B.Z., X.Y.G., X.Z., Y.L.L., Z.L.Q., and C.D. analyzed the data. J.F.G. provided useful insights and reagents. Y.B.Z. and X.Y.G. wrote the manuscript. All authors have read and approved this manuscript.

DECLARATION OF INTERESTS

The authors declare no competing interests.

Received: January 29, 2022
Revised: April 10, 2022
Accepted: July 19, 2022
Published: August 19, 2022

REFERENCES

An, L.L., Zhao, X., Gong, X.Y., Li, Y.L., Qu, Z.L., Sun, H.Y., Guo, W.H., Dan, C., Gui, J.F., and Zhang, Y.B. (2022). Promoter binding and nuclear retention features of zebrafish IRF family members in IFN response. Front. Immunol. *13*, 861262. https://doi.org/10.3389/fimmu.2022.861262.

Bamming, D., and Horvath, C.M. (2009). Regulation of signal transduction by enzymatically inactive antiviral RNA helicase proteins MDA5, RIG-I, and LGP2. J. Biol. Chem. *284*, 9700–9712. https://doi.org/10.1074/jbc.M807365200.

Bergan, V., Kileng, Ø., Sun, B., and Robertsen, B. (2010). Regulation and function of interferon regulatory factors of Atlantic salmon. Mol. Immunol. *47*, 2005–2014. https://doi.org/10.1016/j.molimm.2010.04.015.

Biacchesi, S., Mérour, E., Lamoureux, A., Bernard, J., and Brémont, M. (2012). Both STING and MAVS fish orthologs contribute to the induction of interferon mediated by RIG-I. PLoS One *7*, e47737. https://doi.org/10.1371/journal.pone.0047737.

Bruns, A.M., and Horvath, C.M. (2015). LGP2 synergy with MDA5 in RLR-mediated RNA recognition and antiviral signaling. Cytokine *74*, 198–206. https://doi.org/10.1016/j.cyto.2015.02.010.

Bruns, A.M., Leser, G.P., Lamb, R.A., and Horvath, C.M. (2014). The innate immune sensor LGP2 activates antiviral signaling by regulating MDA5-RNA interaction and filament assembly. Mol. Cell *55*, 771–781. https://doi.org/10.1016/j.molcel.2014.07.003.

Bruns, A.M., Pollpeter, D., Hadizadeh, N., Myong, S., Marko, J.F., and Horvath, C.M. (2013). ATP hydrolysis enhances RNA recognition and antiviral signal transduction by the innate immune sensor, laboratory of genetics and physiology 2 (LGP2). J. Biol. Chem. *288*, 938–946. https://doi.org/10.1074/jbc.M112.424416.

Cadena, C., Ahmad, S., Xavier, A., Willemsen, J., Park, S., Park, J.W., Oh, S.W., Fujita, T., Hou, F., Binder, M., and Hur, S. (2019). Ubiquitin-dependent and -independent roles of E3 ligase RIPLET in innate immunity. Cell *177*, 1187–1200.e16. https://doi.org/10.1016/j.cell.2019.03.017.

Chang, M., Collet, B., Nie, P., Lester, K., Campbell, S., Secombes, C.J., and Zou, J. (2011). Expression and functional characterization of the RIG-I-like receptors MDA5 and LGP2 in Rainbow trout (Oncorhynchus mykiss). J. Virol. *85*, 8403–8412. https://doi.org/10.1128/JVI.00445-10.

Chen, M.R., Chen, H.X., and Yi, Y.L. (1985). The establishment of a heteroploid line from crucian carp and its biological characterisitics. J. Fish. China *9*, 121–130.

Childs, K.S., Randall, R.E., and Goodbourn, S. (2013). LGP2 plays a critical role in sensitizing mda-5 to activation by double-stranded RNA. PLoS One *8*, e64202. https://doi.org/10.1371/journal.pone.0064202.

Chopy, D., Pothlichet, J., Lafage, M., Mégret, F., Fiette, L., Si-Tahar, M., and Lafon, M. (2011).

Ambivalent role of the innate immune response in rabies virus pathogenesis. J. Virol. *85*, 6657–6668. https://doi.org/10.1128/JVI.00302-11.

Duic, I., Tadakuma, H., Harada, Y., Yamaue, R., Deguchi, K., Suzuki, Y., Yoshimura, S.H., Kato, H., Takeyasu, K., and Fujita, T. (2020). Viral RNA recognition by LGP2 and MDA5, and activation of signaling through step-by-step conformational changes. Nucleic Acids Res. *48*, 11664–11674. https://doi.org/10.1093/nar/gkaa935.

Esser-Nobis, K., Hatfield, L.D., and Gale, M., Jr. (2020). Spatiotemporal dynamics of innate immune signaling via RIG-I-like receptors. Proc. Natl. Acad. Sci. USA *117*, 15778–15788. https://doi.org/10.1073/pnas.1921861117.

Feng, H., Zhang, Q.M., Zhang, Y.B., Li, Z., Zhang, J., Xiong, Y.W., Wu, M., and Gui, J.F. (2016). Zebrafish IRF1, IRF3, and IRF7 differentially regulate IFNPhi1 and IFNPhi3 expression through assembly of homo- or heteroprotein complexes. J. Immunol. *197*, 1893–1904. https://doi.org/10.4049/jimmunol.1600159.

Feng, H., Zhang, Y.B., Gui, J.F., Lemon, S.M., and Yamane, D. (2021). Interferon regulatory factor 1 (IRF1) and anti-pathogen innate immune responses. PLoS Pathog. *17*, e1009220. https://doi.org/10.1371/journal.ppat.1009220.

Feng, H., Zhang, Y.B., Zhang, Q.M., Li, Z., Zhang, Q.Y., and Gui, J.F. (2015). Zebrafish IRF1 regulates IFN antiviral response through binding to IFNvarphi1 and IFNvarphi3 promoters downstream of MyD88 signaling. J. Immunol. *194*, 1225–1238. https://doi.org/10.4049/jimmunol.1402415.

Gao, D., Ciancanelli, M.J., Zhang, P., Harschnitz, O., Bondet, V., Hasek, M., Chen, J., Mu, X., Itan, Y., Cobat, A., et al. (2021). TLR3 controls constitutive IFN-beta antiviral immunity in human fibroblasts and cortical neurons. J. Clin. Invest. *131*, e134529. https://doi.org/10.1172/JCI134529.

Gao, L.y., Liu, H., Shi, X.j., He, J.q., and Jiang, Y.L. (2009). Comparison of characteristics of SVCV strains isolated in China and in Europe. Chin. J. Virol. *25*, 47–51.

Gong, X.Y., Zhang, Q.M., Gui, J.F., and Zhang, Y.B. (2019). SVCV infection triggers fish IFN response through RLR signaling pathway. Fish Shellfish Immunol. *86*, 1058–1063. https://doi.org/10.1016/j.fsi.2018.12.063.

Gough, D.J., Messina, N.L., Clarke, C.J.P., Johnstone, R.W., and Levy, D.E. (2012). Constitutive type I interferon modulates homeostatic balance through tonic signaling. Immunity *36*, 166–174. https://doi.org/10.1016/j.immuni.2012.01.011.

Iliev, D.B., Sobhkhez, M., Fremmerlid, K., and Jørgensen, J.B. (2011). MyD88 interacts with interferon regulatory factor (IRF) 3 and IRF7 in Atlantic salmon (Salmo salar): transgenic SsMyD88 modulates the IRF-induced type I interferon response and accumulates in aggresomes. J. Biol. Chem. *286*, 42715–42724. https://doi.org/10.1074/jbc.M111.293969.

Komuro, A., and Horvath, C.M. (2006). RNA- and virus-independent inhibition of antiviral signaling by RNA helicase LGP2. J. Virol. *80*, 12332–12342. https://doi.org/10.1128/JVI.01325-06.

Lam, S.H., Chua, H.L., Gong, Z., Lam, T.J., and Sin, Y.M. (2004). Development and maturation of the immune system in zebrafish, Danio rerio: a gene expression profiling, in situ hybridization and immunological study. Dev. Comp. Immunol. *28*, 9–28. https://doi.org/10.1016/s0145-305x(03)00103-4.

Lenoir, J.J., Parisien, J.P., and Horvath, C.M. (2021). Immune regulator LGP2 targets Ubc13/UBE2N to mediate widespread interference with K63 polyubiquitination and NF-kappaB activation. Cell Rep. *37*, 110175. https://doi.org/10.1016/j.celrep.2021.110175.

Liu, J., Li, J., Xiao, J., Chen, H., Lu, L., Wang, X., Tian, Y., and Feng, H. (2017a). The antiviral signaling mediated by black carp MDA5 is positively regulated by LGP2. Fish Shellfish Immunol. *66*, 360–371. https://doi.org/10.1016/j.fsi.2017.05.035.

Liu, T.K., Zhang, Y.B., Liu, Y., Sun, F., and Gui, J.F. (2011). Cooperative roles of fish protein kinase containing Z-DNA binding domains and double-stranded RNA-dependent protein kinase in interferon-mediated antiviral response. J. Virol. *85*, 12769–12780. https://doi.org/10.1128/JVI.05849-11.

Liu, Y., Qu, L., Liu, Y., Roizman, B., and Zhou, G.G. (2017b). PUM1 is a biphasic negative regulator of innate immunity genes by suppressing LGP2. Proc. Natl. Acad. Sci. USA *114*, E6902–E6911. https://doi.org/10.1073/pnas.1708713114.

Ohtani, M., Hikima, J.i., Kondo, H., Hirono, I., Jung, T.S., and Aoki, T. (2010). Evolutional conservation of molecular structure and antiviral function of a viral RNA receptor, LGP2, in Japanese flounder, Paralichthys olivaceus. J. Immunol. *185*, 7507–7517. https://doi.org/10.4049/jimmunol.1001850.

Parisien, J.P., Lenoir, J.J., Mandhana, R., Rodriguez, K.R., Qian, K., Bruns, A.M., and Horvath, C.M. (2018). RNA sensor LGP2 inhibits TRAF ubiquitin ligase to negatively regulate innate immune signaling. EMBO Rep. *19*, e45176. https://doi.org/10.15252/embr.201745176.

Pippig, D.A., Hellmuth, J.C., Cui, S., Kirchhofer, A., Lammens, K., Lammens, A., Schmidt, A., Rothenfusser, S., and Hopfner, K.P. (2009). The regulatory domain of the RIG-I family ATPase LGP2 senses double-stranded RNA. Nucleic Acids Res. *37*, 2014–2025. https://doi.org/10.1093/nar/gkp059.

Quicke, K.M., Kim, K.Y., Horvath, C.M., and Suthar, M.S. (2019). RNA helicase LGP2 negatively regulates RIG-I signaling by preventing TRIM25-mediated caspase activation and recruitment domain ubiquitination. J. Interferon Cytokine Res. *39*, 669–683. https://doi.org/10.1089/jir.2019.0059.

Rao, Y., Wan, Q., Yang, C., and Su, J. (2017). Grass carp laboratory of genetics and physiology 2 serves as a negative regulator in retinoic acid-inducible gene I- and melanoma differentiation-associated gene 5-mediated antiviral signaling in resting state and early stage of grass carp reovirus infection. Front. Immunol. *8*, 352. https://doi.org/10.3389/fimmu.2017.00352.

Rehwinkel, J., and Gack, M.U. (2020). RIG-I-like receptors: their regulation and roles in RNA sensing. Nat. Rev. Immunol. *20*, 537–551. https://doi.org/10.1038/s41577-020-0288-3.

Rothenfusser, S., Goutagny, N., DiPerna, G., Gong, M., Monks, B.G., Schoenemeyer, A., Yamamoto, M., Akira, S., and Fitzgerald, K.A. (2005). The RNA helicase Lgp2 inhibits TLR-independent sensing of viral replication by retinoic acid-inducible gene-I. J. Immunol. *175*, 5260–5268. https://doi.org/10.4049/jimmunol.175.8.5260.

Saito, T., Hirai, R., Loo, Y.M., Owen, D., Johnson, C.L., Sinha, S.C., Akira, S., Fujita, T., and Gale, M., Jr. (2007). Regulation of innate antiviral defenses through a shared repressor domain in RIG-I and LGP2. Proc. Natl. Acad. Sci. USA *104*, 582–587. https://doi.org/10.1073/pnas.0606699104.

Sanchez David, R.Y., Combredet, C., Najburg, V., Millot, G.A., Beauclair, G., Schwikowski, B., Léger, T., Camadro, J.M., Jacob, Y., Bellalou, J., et al. (2019). LGP2 binds to PACT to regulate RIG-I- and MDA5-mediated antiviral responses. Sci. Signal. *12*, eaar3993. https://doi.org/10.1126/scisignal.aar3993.

Sanders, G.E., Batts, W.N., and Winton, J.R. (2003). Susceptibility of zebrafish (Danio rerio) to a model pathogen, spring viremia of carp virus. Comp. Med. *53*, 514–521.

Satoh, T., Kato, H., Kumagai, Y., Yoneyama, M., Sato, S., Matsushita, K., Tsujimura, T., Fujita, T., Akira, S., and Takeuchi, O. (2010). LGP2 is a positive regulator of RIG-I- and MDA5-mediated antiviral responses. Proc. Natl. Acad. Sci. USA *107*, 1512–1517. https://doi.org/10.1073/pnas.0912986107.

Si-Tahar, M., Blanc, F., Furio, L., Chopy, D., Balloy, V., Lafon, M., Chignard, M., Fiette, L., Langa, F., Charneau, P., and Pothlichet, J. (2014). Protective role of LGP2 in influenza virus pathogenesis. J. Infect. Dis. *210*, 214–223. https://doi.org/10.1093/infdis/jiu076.

Stok, J.E., Oosenbrug, T., ter Haar, L.R., Gravekamp, D., Bromley, C.P., Zelenay, S., Reis E Sousa, C., and van der Veen, A.G. (2022). RNA sensing via the RIG-I-like receptor LGP2 is essential for the induction of a type I IFN response in ADAR1 deficiency. EMBO J. *41*, e109760. https://doi.org/10.15252/embj.2021109760.

Sun, F., Zhang, Y.B., Liu, T.K., Gan, L., Yu, F.F., Liu, Y., and Gui, J.F. (2010). Characterization of fish IRF3 as an IFN-inducible protein reveals evolving regulation of IFN response in vertebrates. J. Immunol. *185*, 7573–7582. https://doi.org/10.4049/jimmunol.1002401.

Sun, F., Zhang, Y.B., Liu, T.K., Shi, J., Wang, B., and Gui, J.F. (2011). Fish MITA serves as a mediator for distinct fish IFN gene activation dependent on IRF3 or IRF7. J. Immunol. *187*, 2531–2539. Epub 2011 Jul 27. https://doi.org/10.4049/jimmunol.1100642.

Suthar, M.S., Ramos, H.J., Brassil, M.M., Netland, J., Chappell, C.P., Blahnik, G., McMillan, A., Diamond, M.S., Clark, E.A., Bevan, M.J., and Gale, M., Jr. (2012). The RIG-I-like receptor LGP2 controls CD8(+) T cell survival and fitness. Immunity *37*, 235–248. https://doi.org/10.1016/j.immuni.2012.07.004.

Takahashi, T., Nakano, Y., Onomoto, K., Yoneyama, M., and Ui-Tei, K. (2020). LGP2 virus sensor enhances apoptosis by upregulating apoptosis regulatory genes through TRBP-bound miRNAs during viral infection. Nucleic Acids Res. *48*, 1494–1507. https://doi.org/10.1093/nar/gkz1143.

Traver, D., Herbomel, P., Patton, E.E., Murphey, R.D., Yoder, J.A., Litman, G.W., Catic, A., Amemiya, C.T., Zon, L.I., and Trede, N.S. (2003). The zebrafish as a model organism to study development of the immune system. Adv. Immunol. *81*, 253–330.

Uchikawa, E., Lethier, M., Malet, H., Brunel, J., Gerlier, D., and Cusack, S. (2016). Structural analysis of dsRNA binding to anti-viral pattern recognition receptors LGP2 and MDA5. Mol. Cell *62*, 586–602. https://doi.org/10.1016/j.molcel.2016.04.021.

Varela, M., Figueras, A., and Novoa, B. (2017). Modelling viral infections using zebrafish: innate immune response and antiviral research. Antiviral Res. *139*, 59–68. https://doi.org/10.1016/j.antiviral.2016.12.013.

Venkataraman, T., Valdes, M., Elsby, R., Kakuta, S., Caceres, G., Saijo, S., Iwakura, Y., and Barber, G.N. (2007). Loss of DExD/H box RNA helicase LGP2 manifests disparate antiviral responses. J. Immunol. *178*, 6444–6455. https://doi.org/10.4049/jimmunol.178.10.6444.

Wu, M., Zhao, X., Gong, X.Y., Wang, Y., Gui, J.F., and Zhang, Y.B. (2019). FTRCA1, a species-specific member of finTRIM family, negatively regulates fish IFN response through autophage-lysosomal degradation of TBK1. J. Immunol. *202*, 2407–2420. https://doi.org/10.4049/jimmunol.1801645.

Yang, Y.J., Wang, Y., Li, Z., Zhou, L., and Gui, J.F. (2017). Sequential, divergent, and cooperative requirements of Foxl2a and Foxl2b in ovary development and maintenance of zebrafish. Genetics *205*, 1551–1572. https://doi.org/10.1534/genetics.116.199133.

Yoneyama, M., Kikuchi, M., Matsumoto, K., Imaizumi, T., Miyagishi, M., Taira, K., Foy, E., Loo, Y.M., Gale, M., Jr., Akira, S., et al. (2005). Shared and unique functions of the DExD/H-box helicases RIG-I, MDA5, and LGP2 in antiviral innate immunity. J. Immunol. *175*, 2851–2858. https://doi.org/10.4049/jimmunol.175.5.2851.

Yu, F.-F., Zhang, Y.-B., Liu, T.-K., Liu, Y., Sun, F., Jiang, J., and Gui, J.-F. (2010). Fish virus-induced interferon exerts antiviral function through Stat1 pathway. Mol. Immunol. *47*, 2330–2341. https://doi.org/10.1016/j.molimm.2010.05.282.

Yu, Y., Huang, Y., Yang, Y., Wang, S., Yang, M., Huang, X., and Qin, Q. (2016). Negative regulation of the antiviral response by grouper LGP2 against fish viruses. Fish Shellfish Immunol. *56*, 358–366. https://doi.org/10.1016/j.fsi.2016.07.015.

Zhang, J., Zhang, Y.B., Wu, M., Wang, B., Chen, C., and Gui, J.F. (2014). Fish MAVS is involved in RLR pathway-mediated IFN response. Fish Shellfish Immunol. *41*, 222–230. https://doi.org/10.1016/j.fsi.2014.09.002.

Zhang, Q.M., Zhao, X., Li, Z., Wu, M., Gui, J.F., and Zhang, Y.B. (2018). Alternative splicing transcripts of zebrafish LGP2 gene differentially contribute to IFN antiviral response. J. Immunol. *200*, 688–703. https://doi.org/10.4049/jimmunol.1701388.

Zhang, Y.B., and Gui, J.F. (2012). Molecular regulation of interferon antiviral response in fish. Dev. Comp. Immunol. *38*, 193–202. https://doi.org/10.1016/j.dci.2012.06.003.

STAR★METHODS

KEY RESOURCES TABLE

REAGENT or RESOURCE	SOURCE	IDENTIFIER
Antibodies		
HA-Tag Rabbit mAb	Cell Signaling Technology	Cat# 3724; RRID:AB_1549585
FLAG Tag Rabbit mAb	Cell Signaling Technology	Cat# 70,569; RRID:AB_2799786
Myc-tag Rabbit mAb	Cell Signaling Technology	Cat# 2040; RRID:AB_2148465
α-Tubulin Rabbit mAb	Cell Signaling Technology	Cat# 2125; RRID:AB_2619646
Lamin A/C Rabbit mAb	Cell Signaling Technology	Cat# 2032; RRID:AB_2136278
CaIRF3 Rabbit mAb	(Sun et al., 2010)	N/A
CaIRF7 Rabbit mAb	(An et al., 2022)	N/A
CaPKR Rabbit mAb	(Liu et al., 2011)	N/A
Zebrafish LGP2 Rabbit mAb	In this study	N/A
Bacterial and virus strains		
Spring viraemia of carp virus (SVCV)	(Gao et al., 2009)	N/A
Chemicals, peptides, and recombinant proteins		
Protease Inhibitor Cocktail	Bimake	Cat# B14002
Phosphatase Inhibitor Cocktail	Bimake	Cat# B15001
Cycloheximide	KH	Cat# A1410
Actinomycin D	KH	Cat# C7698; CAS: 50-76-0
poly(I:C)	SIGMA	Cat# P0913; CAS: 42,424-50-0
Critical commercial assays		
Endo-free Plasmid Mini Kit II	OMEGA	Cat# D6950-02
SV Total RNA Isolation	Promega	Cat# Z3100
GoScript™ Reverse Transcription System	Promega	Cat# A5001
Universal Blue qPCR SYBR Green Master Mix	YEASEN, China	Cat# 11201ES08
Dual-Luciferase® Reporter Assay System	Promega	Cat# P0913
Nuclear and Cytoplasmic Protein Extraction Kit	YEASEN, China	Cat# 20126ES50
ANTI-FLAG(R) M2 Affinity Gel	Sigma	Cat# A2220
Deposited data		
Raw and analyzed data	This paper	Lead Contact, Yibing Zhang (ybzhang@ihb.ac.cn)
Experimental models: Cell lines		
HEK293T	ATCC (CRL-3216)	N/A
Epithelioma papulosum cyprini cells (EPC)	ATCC (CRL-2872)	N/A
Ovary cells of grass carp (CO)	Kept in IHB,CAS	N/A
Crucian carp (*C. auratus L.*) blastulae embryonic cells (CAB)	(Chen et al., 1985)	N/A
Zebrafish liver cells (ZFL)	ATCC, CRL2643	N/A
Experimental models: Organisms/strains		
Zebrafish (*Danio rerio*) strain AB	China Zebrafish Resource Center	N/A

(*Continued on next page*)

Continued

REAGENT or RESOURCE	SOURCE	IDENTIFIER
Oligonucleotides: see Table S1		
Recombinant DNA		
pcDNA3.1(+)	Invitrogen	Cat# V79020
pcDNA3.1/myc-His (−)	Invitrogen	Cat# V855-20
Software and algorithms		
GraphPad Prism 8.00	N/A	https://www.graphpad.com/
ImageJ	N/A	https://imagej.nih.gov/ij/
Figdraw	N/A	https://www.figdraw.com/static/index.html#/

RESOURCE AVAILABILITY

Lead contact

Further information and requests for resources and reagents should be directed to and will be fulfilled by the Lead Contact, Yibing Zhang (ybzhang@ihb.ac.cn).

Materials availability

The *lgp2*-deficient zebrafish mutant line and plasmids generated in this study are available from the Lead Contact without restriction.

Data and code availability

Raw and analyzed data reported in this paper will be shared by the lead contact upon request.

This paper does not report original code.

Any additional information required to reanalyze the data reported in this paper is available from the Lead Contact upon request.

EXPERIMENTAL MODEL AND SUBJECT DETAILS

Cell lines and cell culture

Epithelioma papulosum cyprini cells (EPC), zebrafish liver cells (ZFL) and HEK293T cells are from ATCC. Grass carp *C. idellus* ovary cells (CO), and crucian carp (*C. auratus*) blastulae embryonic cells (CAB) are kept in our Institute of Hydrobiology, Chinese Academy of Sciences. EPC, CAB and CO cells were grown in medium 199 (Gibco) supplemented with 10% fetal bovine serum (FBS) at 28°C, and HEK293T cells were cultured in DMEM (Gibco) with 10% FBS at 37 °C.

Virus strains and experimental models

Spring viraemia of carp virus (SVCV), a negative-sense single-stranded RNA virus of the family Rhabdoviridae (Gao et al., 2009), was propagated and tittered in EPC cells by a 50% tissue culture-infective dose ($TCID_{50}$) assay. Zebrafish (*Danio rerio*) strain AB (from China Zebrafish Resource Center) were raised, maintained, reproduced, and staged according to standard protocols, which were approved by the Animal Care and Use Committee of Institute of Hydrobiology, Chinese Academy of Sciences. For *in vivo* infection, zebrafish larvae were immersed with SVCV, and zebrafish adults injected i.p. (intraperitoneally injection) with SVCV.

METHOD DETAILS

Generation of LGP2 mutants by TALEN technique

TALEN design software TAL Effector Nucleotide Targeter 2.0 (https://talent.cac.cornell.edu/) and E-TALEN (http://www.etalen.org/E-TALEN/) were used to design the LGP2 target sites and TALEs recognition sequence. The TALEN pair and spacer sequences were targeted to the exon 10 of zebrafish LGP2 gene as below: TALEN-left: TGTTTGAGCTCCAGAA; TALEN-right: TCAGCCTCCATCCGA; TALEN-spacer: AACAGCTGTGGTGAT, with a site of *Pvu* II. TALEN plasmids were constructed using the "unit assembly method" through assembling the correct sequences into pCS2-FokI, for *in vitro* synthesis of mRNAs

using an SP6 mMessage mMachine kit (Ambion), which were co-injected into the embryos at the one-cell stage at a dose of 500–600 pg per embryo. 24–48 h later, DNA spanning the LGP2 targeting sites were amplified by PCR to evaluate mutation (Yang et al., 2017). LGP2 mutants is resistant to *Pvu* II digestion due to mutations in spacer, which was further confirmed by sequencing. After the F1 of LGP2 mutant was obtained, the mutant male and female fish with the same phenotype were bred to obtain the F2 mutant. The *lgp2*$^{lof/lof}$ mutants are viable, albeit slightly low fertilization rates and slightly small sizes when grown up.

Plasmids

For Co-IP assays, plasmids including zebrafish LGP2-HA, MDA5-HA, RIG-I-HA, TBK1-HA and IKKi-HA were generated by inserting the open reading frames (ORFs) into *EcoR* V site of pcDNA3.1(+) vector (Invitrogen) that had preexisted an HA coding sequence into *Not* I site. Zebrafish LGP2-Myc, MDA5-Myc, MITA-Myc, TBK1-Myc, IRF3-Myc and IRF7-Myc were made by insertion of the corresponding ORFs into *EcoR* I/*BamH* I site of pcDNA3.1/myc-His(−) vector (Invitrogen). The dominant negative mutants of RLR signaling factors, including zebrafish RIG-I-DN, MDA5-DN, MAVS-ΔTM, MITA-CT, TBK1-K38M, IRF3-DN, IRF7-DN, IRF9-ΔC were made previously in our lab (Feng et al., 2015, 2016; Sun et al., 2010, 2011; Wu et al., 2019; Zhang et al., 2018). CaIFNpro-luc was made by insertion of 5′flanking sequence (−233 to +34) of crucian carp *C. auratus* IFN (GenBank accession no. HM187723) into *Kpn* I/*Xho* I sites of pGL3 (Sun et al., 2010). Zebrafish IFNφ1pro-luc was made by insertion of 5′flanking sequence (−586 to +38) of zebrafish IFNφ1 (GenBank accession no. NM_207640) into pGL3 (Sun et al., 2011). For overexpression assays, all plasmids, unless indicated, were expressed as non-tagged proteins.

Transfection and luciferase activity assays

Transfection assays were performed according to our previous reports (Gong et al., 2019; Zhang et al., 2018). Typically, fish cells were seeded overnight in plates, transfected for 24h with various constructs at a ratio of 10:10:1 (promoter-driven luciferase plasmid/expression plasmid/Renilla luciferase plasmid pRL-TK) using with polyethylenimine, linear (PEI, MW25000; Aldrich, 1 μg/μL of storage concentration) according to the manufacturer's instructions. Generally, cells seeded overnight were replenished with the transfection mixture. The transfection mixture was made by diluting the indicated plasmids with Opti-mem (200, 50 and 25μL for each well in 6-, 24- or 48-well plates, respectively), followed by addition of PEI with a ratio of 1:3 [plasmid (μg)/PEI (μL)] for fish cells and 1:5 for HEK293T cells. The doses of transfected plasmids were proportional to the number of fish cells seeded in different plates or dishes. For example, 4-fold doses of the plasmids were transfected in 6-well plates compared to that in 24-well plates (10 ng for low dose of LGP2 and 200 ng for high dose). If necessary, the cells were transfected again with poly(I:C) (SIGMA) or infected with SVCV infection. Luciferase activities were measured by a Junior LB9509 luminometer (Berthold, Pforzheim, Germany), according to the Dual-Luciferase Reporter Assay System (Promega, USA). All results were shown as a representative of at least three independent experiments, each performed in triplicate.

RNA extraction, cDNA synthesis, and quantitative real-time PCR

Total RNA was extracted by TRIZOL Reagent (Promega), followed by removing genomic DNA by RNase-free DNase I. First-strand cDNA was synthesized using random primers or Oligo(dT)$_{20}$VN (Promega). RT-qPCR was performed with Universal Blue qPCR SYBR Green Master Mmix (YEASEN, China) in a DNA Engine Chromo four real-time system (BioRad, USA). Gene expression was normalized to β-actin in a given sample, indicated as relative expression values of mRNA, or further normalized to the control as a fold induction of mRNA. The primers used in this study were listed in Table S1.

Fractionation of nuclear and cytoplasmic proteins

Nuclear and cytoplasmic proteins were extracted according to the manufacturer's protocol (YEASEN, China) (Sun et al., 2010). Cells were collected with cell scrapers, followed by centrifugation. Briefly, cell pellets were added with reagent A containing PMSF, vortexed thoroughly, incubated on ice for 10–15 min, and added with cytoplasmic protein extraction reagent B. After vortex and centrifugation, the supernatants were collected as cytoplasmic proteins. The remained pellets were further incubated with reagent C containing PMSF for 30 min on ice, vortexed thoroughly, and finally centrifuged to obtain nuclear proteins.

Coimmunoprecipitation and western blotting

Coimmunoprecipitation (Co-IP) assays and western blotting were performed as previously described (Feng et al., 2015; Sun et al., 2010, 2011; Zhang et al., 2018). For Coimmunoprecipitation (Co-IP) assays, cells were lysed with NP-40 lysis buffer (Beyotime, China), followed by centrifugation. Cell lysates were incubated with anti-Tag beads (Sigma, USA) at 4°C overnight. The beads were washed with Co-IP wash buffer (50mM Tris-HCl, pH7.5, 150mM NaCl, 1mM DTT, 1% NP-40), resolved in SDS loading buffer (Biosharp, China), followed by western blotting with the indicated antibodies. Tag-specific Abs were purchased from Cell Signaling Technology and ABclonal. Antibodies for CaIRF3, CaIRF7 and CaPKR were described previously (Sun et al., 2010; Zhang et al., 2018). Zebrafish LGP2-specific Ab was generated by immunization of rabbits with a purified peptide corresponding to 192–417 aa of zebrafish LGP2.

QUANTIFICATION AND STATISTICAL ANALYSIS

All quantitative experiments were performed with at least three independent biological repeats unless otherwise indicated. The results were analyzed and graphed using the GraphPad Prism 8 software. Data were shown as mean ± SD (N = 3). P values were calculated using Student's t test. *$p < 0.05$, **$p < 0.01$; n.s., not significant.